2,3,5,6-Tetrakis(methylene)-1,4-cyclohexanediyl (1,2,4,5-Tetramethylenebenzene), a Disjoint Non-Kekulé Singlet Hydrocarbon Biradical

James H. Reynolds,[1a] Jerome A. Berson,*[1a] Kristin K. Kumashiro,[1a] James C. Duchamp,[1a] Kurt W. Zilm,*[1a] J. C. Scaiano,*[1b] Alain B. Berinstain,[1b] Albino Rubello,[1c] and Pierre Vogel*[1c]

Contribution from the Department of Chemistry, Yale University, New Haven, Connecticut 06511, Ottawa–Carleton Chemistry Institute, University of Ottawa Campus, Ottawa, Canada K1N 6N5, and Institute of Organic Chemistry, University of Lausanne, Lausanne, Switzerland CH-1005

Received March 25, 1993

Abstract: The title compound **4a**, a purple transient whose main UV–vis absorption band occurs near 490 nm (ϵ = 5000 M^{-1} cm^{-1}), has been generated by irradiation of 2,3,5,6-tetramethylene-7-oxonorbornane (**5a**). It has been observed directly by immobilization in frozen matrices or in polymer films and by time-resolved spectroscopy following nanosecond laser flash photolysis of the ketone precursor **5a**. Although the matrix-immobilized irradiated samples containing biradical **4a** show a triplet electron spin resonance (ESR) spectrum at low temperature, some other species is the carrier, since the ESR spectrum persists even after complete photobleaching of the UV–vis spectrum characteristic of **4a**. The singlet spin state for biradical **4a**, predicted by theory, is confirmed not only by the absence of an ESR spectrum assignable to it but also by the appearance of a ^{13}C cross-polarization magic angle spinning NMR spectrum (δ = 113 ppm) observed when glassy preparations of **5a**-*2,3-di-$^{13}CH_2$* are irradiated. The rates of dimerization of **4a** in fluid media, (1.9–3) × 10^{10} M^{-1} s^{-1}, and the rate of capture by O_2, 1.86 × 10^7 M^{-1} s^{-1}, are also consistent with the behavior expected of a singlet biradical.

Whether the spin state of a π-conjugated non-Kekulé species can be predicted from its structure has been a contentious issue since 1936.[2] Müller and Bunge,[3] citing Hund,[4a–c] invoked a generalized version of Hund's high-spin rule[4d] to claim concordance with theory in their finding of triplet states of both of the Schlenk–Brauns[5] hydrocarbons **1** and **2**. On the other hand, Hückel[6] pointed out that because of a subtle difference in structure, the exchange energy of **2** should be much smaller than that of **1** and, therefore, **2** might violate the rule by preferring to exist as a singlet species.

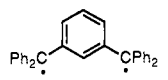

1

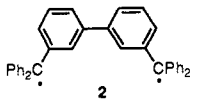

2

Hückel's argument can be generalized by the statement that *the connectivity of the atoms of the π-framework of a conjugated non-Kekulé species is a strong determinant of the energy separation between the lowest spin states.* Although several modern derivations of this formulation have become available,[7,8] perhaps the clearest comes from the insight of Borden and Davidson[9] that the structure of one class of π-conjugated hydrocarbon biradicals permits the two nominally nonbonding electrons to reside in "disjoint" molecular orbitals, confinable to separate spatial domains. Therefore, in a first-order approximation, the exchange energies of the singlet and triplet do not differ and a higher order effect, dynamic spin polarization, should favor the singlet.

Detailed quantum mechanical calculations confirm these ideas, but agreement with experiment has been problematic. The prototype of such disjoint hydrocarbon species is tetramethyleneethane (**3**), a molecule that can be constructed mentally by the union of two allyl radicals at inactive sites. Several levels of ab initio computation applied to this molecule predict a small (1–2 kcal/mol) preference for a singlet ground state, in accord with the qualitative predictions of the disjoint model.[9,10] These predictions, however, conflict with the experimental assignment[11] of a triplet ground state to the molecule, and a more recent calculation[12] predicts that a triplet ground state at its optimized geometry should be favored by 1.0–1.5 kcal/mol.

3

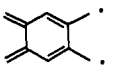

4

Although the apparent discrepancies in the case of **3** might be blamed on a hypothetical inability of even a high level of theory to deal properly with such a small gap, one's confidence in the entire disjoint concept must be shaken by the apparently incorrect prediction of a singlet in the case of tetramethylenebenzene (TMB) **4**. This disjoint hydrocarbon can be derived by the union of two pentadienyl radicals at inactive sites and is predicted by semiem-

(1) (a) Department of Chemistry, Yale University. (b) Ottawa–Carleton Chemistry Institute. (c) University of Lausanne.

(2) For reviews, see: (a) Berson, J. A. In *The Chemistry of the Quinonoid Compounds*; Patai, S., Rappoport, Z., Eds; Wiley,: New York, 1988; Vol 2, Part 1, p 195. (b) Berson, J. A. *Mol. Cryst. Liq. Cryst.* **1989**, *176*, 1.

(3) Müller, E.; Bunge, W. *Ber. Dtsch. Chem. Ges.* **1936**, *69*, 2168.

(4) (a) Hund, F. Personal communication cited in ref 3. (b) Hund, F. *Linienspektren Periodisches System der Elemente*; Springer-Verlag: Berlin, 1927; p 124ff. (c) Hund, F. *Z. Phys.* **1928**, *51*, 759. (d) See also: Longuet-Higgins, H. C. *J. Chem. Phys.* **1950**, *18*, 265.

(5) Schlenk, W.; Brauns, M. *Ber. Dtsch. Chem. Ges.* **1915**, *48*, 661, 716.

(6) Hückel, E. *Z. Phys. Chem., Abt. B* **1936**, *34* 339.

(7) (a) Ovchinnikov, A. A. *Theor. Chim. Acta* **1978**, *47*, 497. (b) Misurkin, I. A.; Ovchinnikov, A. A. *Russ. Chem. Rev. (Engl. Transl.)* **1977**, *46*, 967.

(8) (a) See, for example: Seeger, D. E.; Lahti, P. M.; Rossi, A. R.; Berson, J. A. *J. Am. Chem. Soc.* **1986**, *108*, 1251 and references cited therein. (b) For a recent discussion on the interrelations of connectivity, spin density, and the singlet–triplet gap, see: Prasad, B. L. V.; Radhakrishnan, T. P. *J. Phys. Chem.* **1992**, *96*, 9232.

(9) Borden, W. T.; Davidson, E. R. *J. Am. Chem. Soc.* **1977**, *99*, 4587.

(10) (a) Du, P.; Borden, W. T. *J. Am. Chem. Soc.* **1987**, *109*, 930. (b) Nachtigall, P.; Jordan, K. D. *J. Am. Chem. Soc.* **1992**, *114*, 4743.

(11) Dowd, P.; Chang, W.; Paik, Y. H. *J. Am. Chem. Soc.* **1986**, *108*, 7416.

(12) Nachtigall, P.; Jordan, K. D. *J. Am. Chem. Soc.* **1993**, *115*, 270.

0002-7863/93/1515-8073$04.00/0

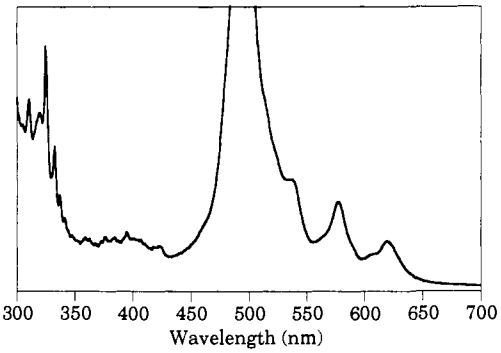

Figure 1. UV–vis absorption spectrum of the TMB transient **4a** obtained by irradiation of ketone **5a** in 2-MTHF at 77 K. The vertical axis shows optical density.

pirical[13] and ab initio[14,15] theory to have a singlet ground state. Several high levels of ab initio theory predict the singlet to be favored by 5–7 kcal/mol,[15] and yet, experiment has led to the assignment[16,17] of a triplet ground state.

The present paper[18] reconsiders previous[16,17] experimental evidence on TMB and adds several new findings. First, it shows that the ESR and UV–vis spectra previously[16] attributed to TMB, in fact, do not arise from a common species. Second, it identifies the carrier of the UV–vis spectrum as a singlet state of TMB. These observations remove the conflict between theory and experiment in the TMB case and strongly support the disjoint hypothesis.

Syntheses of 2,3,5,6-Tetramethylidenebicyclo[2.2.1]heptan-7-one (7-Oxa[2.2.1]hericene, 5a) and 7-Oxa[2.2.1]hericene-*2,3-dimethylidene-^{13}C* (5b), Precursors of TMB 4a and TMB-*2,3-dimethylidene-^{13}C* 4b. The original Rubello–Vogel synthesis[19] of **5a** from tetraester **6a** was repeated in the Yale laboratories[20] in an overall yield of 2.8%. For the preparation of the ^{13}C-labeled species **4b**, the synthesis of precursor **5b** by the method of Roth and co-workers[16] proved to be more convenient. Details are given in the supplementary material to our earlier communication[18a] and elsewhere.[20]

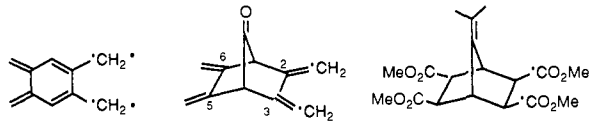

a: •CH_2 unlabeled
b: •CH_2 ^{13}C labeled

Photochemical Generation of Biradical 4. UV–Vis and IR Spectroscopic Characterization. Pyrex-filtered ($\lambda > 300$ nm) photolysis of ketone **5a** immobilized in a 2-methyltetrahydrofuran (2-MTHF) glass at 77 K generated an intensely purple species which showed (Figure 1) a strong absorption band at 490 nm. Other bands appeared on either side of the main transition (strong bands at 332 and 325 nm, weak bands at 575 and 620 nm, and a shoulder at 535 nm). A strong continuous absorption dominated the region below 300 nm. These features match those reported by others.[16] The carrier of the UV–vis spectrum is a transient species, since thawing the matrix caused the irreversible disappearance of the color and the spectrum.

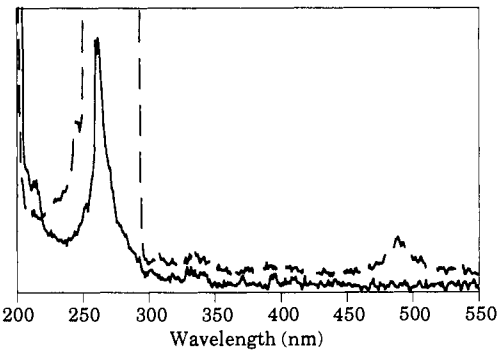

Figure 2. UV–vis spectra of glassy preparations of ketone **5a** (0.4 mM) in methylcyclohexane at 77 K: (—) prior to photolysis; (– —) after 15 s of Pyrex-filtered *hν*.

Table I. Position of the λ_{max} of 1,2,4,5-Tetramethylenebenzene (**4a**) under Various Conditions

conditions	λ_{max} (nm)
2-methyltetrahydrofuran, glass, 15–77 K	490
methylcyclohexane, glass, 77 K	492
diethyl ether, glass, 77 K	490
ethanol/methanol (4/1), glass, 77 K	488
toluene, glass, 77 K	490
poly(methyl methacrylate), thin film, 77–195 K	487
chloroform, solution, 291 K[a]	485

[a] Determined by laser flash photolysis in $CHCl_3$ solution.

All of the absorption bands appeared to grow in at the same rate when a sample of ketone **5a** was irradiated in 5-min increments at 14 K in 2-MTHF. This is consistent with a single species as the carrier of the observed spectrum. Fluorescence excitation–emission spectra and time-resolved flash photolysis kinetic experiments, to be described, provide confirmatory evidence.

In addition to the sharp bands at 332 and 325 nm, other strong transitions appeared at shorter wavelengths, in the region of 260–300 nm, by irradiation of a dilute ($\sim 4 \times 10^{-4}$ M) sample of ketone **5a** in methylcyclohexane at 77 K for a brief period (Figure 2). These bands appeared after less than 5 s of photolysis time and were visible even before the absorption at 490 nm emerged. The intensity of the 260–300-nm absorptions quickly exceeded the detection limits of the spectrometer, so it was difficult to correlate their growth with the absorptions in the visible region. Because they screened the π, π^*-absorption of ketone **5a** (λ_{max} = 260 nm, ϵ = 13 000), these short-wavelength peaks acted as an internal filter which limited the extent of photoconversion **5a** → **4a**, especially at higher initial concentrations of ketone.

The band positions described were nearly independent of solvent (Table I). Although ketone **5a** forms hemiketals in hydroxylic solvents, the ketalization is slow enough to permit the generation of a spectrum of the purple transient by irradiation of a 4:1 ethanol/methanol glassy solution at 77 K. The spectrum also showed no thermochromism, remaining unchanged in 2-MTHF between 14 and 77 K and in poly(methyl methacrylate) between 77 and 195 K.

The main features of the UV–vis spectrum of the purple transient in organic glasses are essentially the same as those reported by Roth and co-workers[16] for specimens in an argon matrix, except that in argon, the main band is blue-shifted to 475 nm and additional fine structure, not observable in the frozen solvents, is seen scattered in the regions of the 570- and 620-nm bands.

We obtained the extinction coefficients of the bands of the purple transient on samples of ketone **5a** that had been photolyzed to "complete" conversion. The supplementary material gives a

(13) (a) Lahti, P. M.; Rossi, A.; Berson, J. A. *J. Am. Chem. Soc.* **1985**, *107*, 2273. (b) Lahti, P. M.; Ichimura, A. S.; Berson, J. A. *J. Org. Chem.* **1989**, *54*, 958.
(14) Lahti, P. M.; Rossi, A.; Berson, J. A. *J. Am. Chem. Soc.* **1985**, *107*, 4362.
(15) Du, P.; Hrovat, D. A.; Borden, W. T.; Lahti, P. M.; Rossi, A. R.; Berson, J. A. *J. Am. Chem. Soc.* **1986**, *108*, 5072.
(16) Roth, W. R.; Langer, R.; Bartmann, M.; Stevermann, B.; Maier, G.; Reisenauer, H. P.; Sustmann, R.; Müller, W. *Angew. Chem., Int. Ed. Engl.* **1987**, *26*, 256.
(17) Roth, W. R.; Langer, R.; Ebbrecht, T.; Beitat, A.; Lennartz, H.-W. *Chem. Ber.* **1991**, *124*, 2751.
(18) For preliminary communications, see: (a) Reynolds, J. H.; Berson, J. A.; Kumashiro, K. K.; Duchamp, J. C.; Zilm, K. W.; Rubello, A.; Vogel, P. *J. Am. Chem. Soc.* **1992**, *114*, 763. (b) Reynolds, J. H.; Berson, J. A.; Scaiano, J. C.; Berinstain, A. B. *J. Am. Chem. Soc.* **1992**, *114*, 5866.
(19) Rubello, A.; Vogel, P. *Helv. Chim. Acta* **1988**, *71*, 1268.
(20) Reynolds, J. H. Ph.D. Thesis, Yale University, New Haven, CT, 1993.

discussion of the estimated errors of about 20% in these determinations.

Ab initio theoretical calculations on TMB[15] predict that the *singlet* should show an intense, longest wavelength band to the red of 416 nm with $f \sim 0.076$ due to the dipole-allowed $^1A_g \rightarrow {}^1B_{3u}$ transition. This seems to be in agreement with the observed 490-nm (f = 0.036 –0.043) band, but the calculations do not predict the weak bands observed at 530 (sh), 575, and 620 nm. Since the present work shows the latter features to be authentic to the purple transient, theory, so far, cannot be said to have provided a firm basis for assignment of the spin state on the basis of the optical spectrum. For the *triplet*, the calculations[15] predict an allowed $^3B_{1u} \rightarrow {}^3B_{2g}$ ($\lambda_{max} > 444$ nm, $f \sim 0.059$) and a forbidden $^3B_{1u} \rightarrow {}^3B_{3u}$ (570 nm) transition. Here, the match with part of the observed spectrum is somewhat better than that of the singlet, but, again, theory fails to predict the extra transitions at 530 and 620 nm. Although this match has been interpreted[16] as favoring the assignment of a triplet ground state, in our view, the calculations at this time raise more questions than they answer. Further theoretical studies, incorporating σ–π-interactions[15] and guided by experimental knowledge of the polarizations of the transitions, are needed. In the meantime, we cannot rely upon the available computational results on the optical spectra as diagnostic for the spin for the ground state.

High-Temperature Matrix Immobilization of 1,2,4,5-Tetramethylenebenzene. In glassy matrices at 77 K, the intensity of the UV–vis absorption of the purple transient remains undiminished for many days. To search for thermally accessible species related to the TMB biradical, we incorporated the precursor ketone **5a** into matrices that would keep the species immobilized at temperatures higher than those of the frozen solvent preparations. We incorporated ketone **4a** into polycrystalline adamantane to the extent of 3.5% (NMR analysis) by cosublimation[21] and into a film of poly(methyl methacrylate) by evaporative codeposition from a solution.[22,23]

At 77 K, 313-nm photolysis of the adamantane preparation led to the appearance of a pink color on the surface but the color did not intensify upon irradiation for an additional 20 min, presumably because of scattering of the light by the polycrystalline powder. The color was stable for several hours at 120 K but faded within 1 min at 196 K.

Photolysis of the poly(methyl methacrylate) film samples at 77 K again gave rise to the characteristic color of TMB. Because of the better optical properties of the polymer films, the color was visibly more intense than that obtained from the adamantane samples. Although UV–vis spectroscopy did not detect the long-wavelength features between 530 and 620 nm because of the low optical densities (0.05–0.08) of the films in this region, the 490-nm absorption of TMB was observed readily. The color was stable in the film matrix up to 212 K but faded irreversibly when the sample was warmed to 223 K. This temperature is near that at which the color of films of 3,4-dimethylenefuran and 3,4-dimethylenethiophene faded[23] and appears to be the upper limit of temperature at which poly(methyl methacrylate) remains sufficiently rigid to act as a matrix support. The results of ESR examinations of persistently colored films at lower temperatures are reported below.

Fluorescence Excitation Spectroscopy. Irradiation at the main absorption maximum of the purple TMB transient in 2-MTHF at 77 K produced a strong emission at 670 nm (Figure 3) and weaker bands at 610, 560, and 540 nm. The emission spectrum was roughly the mirror image of the absorption spectrum. The excitation spectrum for the emission, monitored at the 670-nm emission maximum, showed a strong peak at 470 nm and a series of peaks between 520 and 620 nm whose positions were similar to those of the absorption spectrum. The relative intensities of the excitation peaks were slightly different from those of the absorption spectrum. Specifically, the long-wavelength excitation peaks were relatively stronger than those in the absorption spectrum, probably because of higher fluorescence quantum efficiency from the corresponding excited states.[24] Nevertheless, the fact that all of the absorption bands gave rise to the same emission is a strong indicator that they originate from a single species.

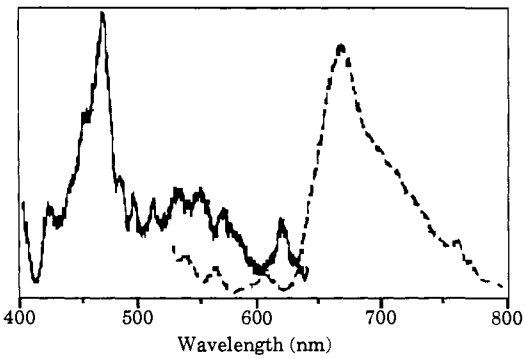

Figure 3. Fluorescence excitation–emission spectra of **4a** in 2-MTHF at 77 K: (—) excitation spectrum (λ_{em} = 670 nm); (– – –) emission spectrum (λ_{ex} = 490 nm).

Matrix-Isolation Infrared Spectroscopy.[25] Sublimation of ketone **5a** into an argon stream which was then deposited onto a CsI window at 20 K gave a matrix-isolated specimen. Irradiation of this sample for 2 h at >300 nm caused about 15% conversion of ketone **5a** to products whose formation was signaled by the new absorptions shown in the difference spectrum of Figure 4.

A strong band of carbon monoxide is apparent at 2133 cm^{-1}. Other bands, prominent among which are those at 1498.1, 849.3, and 807.6 cm^{-1}, also grow in. Inspections of samples at successively longer times of irradiation show that these bands appear at the same rate and, therefore, presumably have a common carrier. The bands at 849.3 and 807.6 cm^{-1}, the strongest in the IR spectrum of TMB, also had been reported (at 854 and 810 cm^{-1}) by Roth and co-workers,[16] who assigned them to out-of-plane C–H bending vibrations by analogy with the corresponding bands reported[26] for the allyl radical. Similarly, the strongest bands for *o*-quinodimethane also appear in the C–H bending region.[26]

Polymerization of TMB in Annealed Matrices. Annealing glassy 2-MTHF preparations of the TMB transient from 77 to 120 K caused striking, visually observable transformations. The purple color of biradical **4a** faded, and the matrices passed through a distinctly yellow phase. This yellow color also disappeared in turn, and as the glass melted at higher temperatures, polymeric material precipitated. These changes were easily monitored by UV–vis spectroscopy.

Annealing ($\sim$100 K) and then refreezing a purple 2-MTHF glass containing irradiated ketone **5a** caused the color and the UV–vis spectrum of biradical **4a** to disappear. A new spectrum appeared which had λ_{max} = 380 nm (Figure 5). This spectrum, including the shoulders at 410 and 355 nm, was nearly identical to that reported[27,28] for *o*-quinodimethane. Moreover, the fluorescence spectrum of the new annealing product (Figure 6) also showed a strong feature centered around 470 nm, which is

(21) Walter, H. F.; Beaudry, W. T.; Camaioni, D. M.; Pratt, D. W. *J. Am. Chem. Soc.* **1985**, *107*, 793.
(22) Radziszewski, J. G.; Burkhalter, F. A.; Michl, J. *J. Am. Chem. Soc.* **1987**, *109*, 61.
(23) (a) Stone, K. J.; Greenberg; M. M.; Blackstock, S. C.; Berson, J. A. *J. Am. Chem. Soc.* **1989**, *111*. 3659. (b)Greenberg, M. M.; Blackstock, S. C.; Stone, K. J.; Berson, J. A. *J. Am. Chem. Soc.* **1989**, *111*, 3671.
(24) (a) Calvert, J. G.; Pitts, J. N., Jr. *Photochemistry*; Wiley: New York, 1966; p 277. (b) Schulman, S. G. *Fluorescence and Phosphorescence Spectroscopy: Physicochemical Principles and Practice*; Pergamon Press: New York, 1977.
(25) We thank D. M. Birney for collaboration in early cryogenic UV and IR experiments.
(26) Maier, G.; Reisenauer, H. P.; Rohde, B.; Dehnicke, K. *Chem. Ber.* **1982**, *116*, 732.
(27) Tseng, K. L.; Michl, J. *J. Am. Chem. Soc.* **1977**, *99*, 4840.
(28) Flynn, C. R.; Michl, J. *J. Am. Chem. Soc.* **1974**, *96*, 3280.

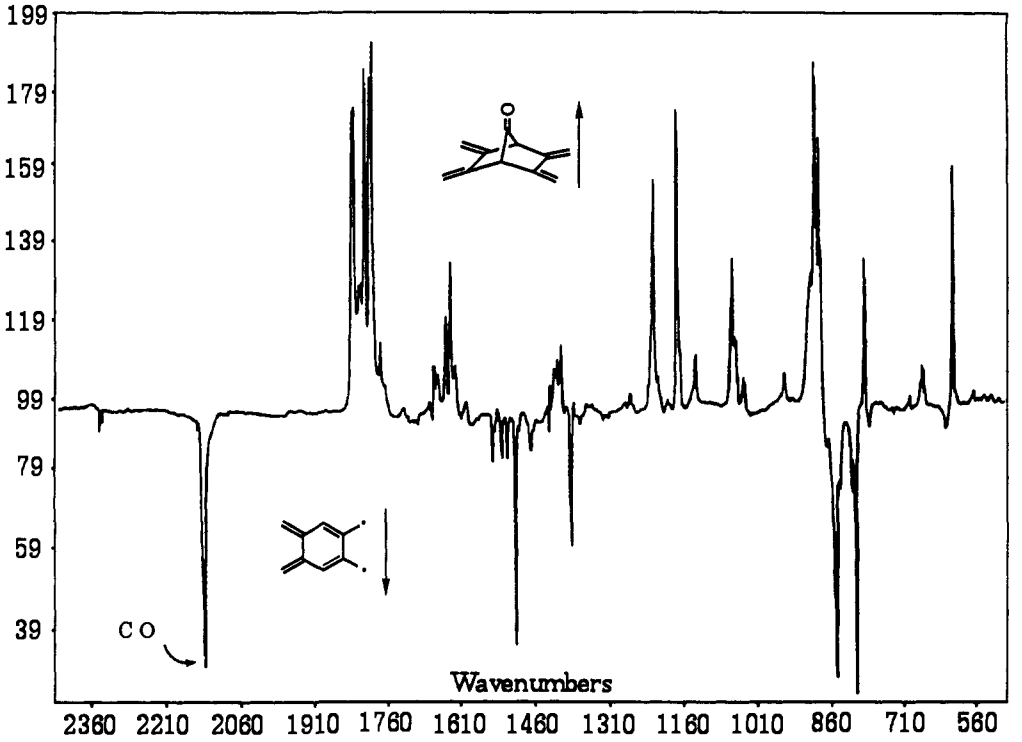

Figure 4. Difference infrared spectrum produced by >300-nm photolysis of ketone **5a** in an argon matrix at 15 K.

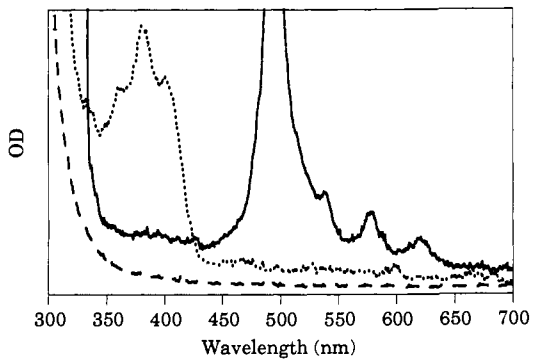

Figure 5. UV–vis spectrum of **4a** in 2-MTHF at 77 K: (—) prior to annealing, (• • •) after annealing the matrix and recooling to 77 K; (– – –) after thawing at room temperature and recooling to 77 K.

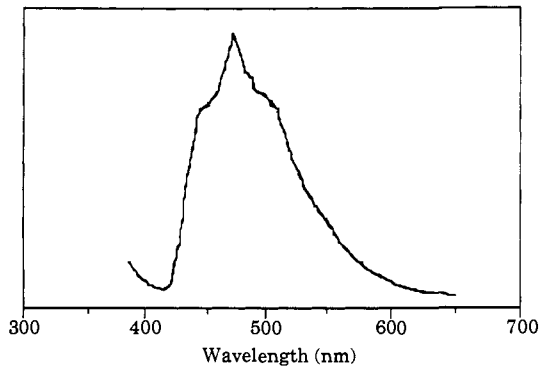

Figure 6. Emission spectrum of the species produced by annealing a 2-MTHF glass containing biradical **4a** (λ_{ex} = 380 nm).

near the position of the fluorescence at 456 nm associated[28] with *o*-quinodimethane.

The intensity of the 380-nm absorption band depended on the extent of matrix annealing; further softening of the glass caused a decrease in the absorption. Complete thawing of the matrix led to the formation of polymer and to the destruction of all long-wavelength (λ > 300 nm) absorptions. Subsequent gas chromatographic (GC) analysis of the solution revealed only

Chart I. Hypothetical Dimers of TMB (**4a**)

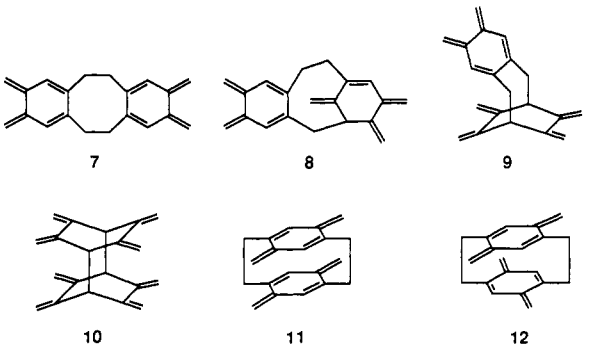

unphotolyzed ketone **5a**. No other low molecular weight species were detected when the material was examined by direct injection mass spectrometry (DIP/MS).

There are several ways to envision the formation of *o*-quinodimethane units in reactions of TMB biradical **4a**. One such process, the intramolecular cyclization to cyclobuta-*o*-quinodimethane, has been observed[16] in the photochemistry of TMB **4a** and will be discussed further in the section that follows. However, the laser flash photolysis experiments, also to be described,[18b] suggest that the decay of **4a** in solution is dominated by a second-order dimerization process. If the same mode of reaction prevails when **4a** is allowed to diffuse in a softened matrix, hypothetical structures (**7–12**) for several plausible TMB dimers can be generated merely by making every sensible bond connection between the radical centers of **4a** (Chart I).

Three of these dimers (**7–9**) contain *o*-quinodimethane units and therefore represent possible carriers of the 380-nm absorption observed in the annealing experiments. The symmetrical dimer **7** and the unsymmetrical anti-Bredt dimer **8** are the counterparts of the dimers formed by 3,4-dimethylenefuran.[23] As we shall show, solution-phase trapping studies of TMB provide evidence that **7** is a major product of TMB dimerization. If this finding can be applied to the annealed matrix experiments, the formation of polymer finds a logical mechanism. Dimer **7** contains *two* highly reactive *o*-quinodimethane units and can react at both ends of the molecule. As reaction of **7** proceeds, the concentration of *o*-quinodimethane units should decrease, in accord with the

Scheme I

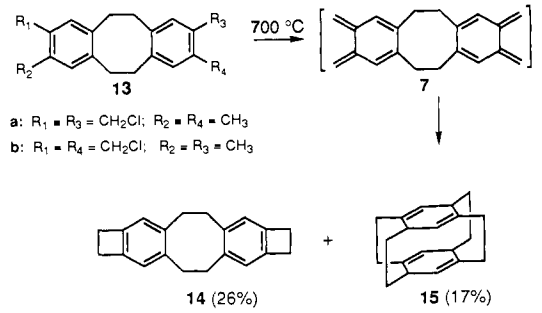

Scheme II

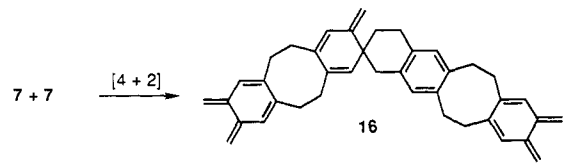

observed decay of the 380-nm absorption. The two *o*-quinodimethane units in **7** serve essentially as chain-propagating sites. In principle, the polymerization could continue indefinitely until terminated either by cyclization or by addition to a species that lacks an *o*-quinodimethane unit. Also, if dimers of TMB other than **7** were produced in the initial dimerization, they also would be incorporated into the growing polymer.

Dimer **7**, although apparently not observed directly heretofore, has been postulated as an intermediate in the gas-phase pyrolyses of dichlorides **13a** and **13b**, which give the bis(cyclobutabenzene) derivative **14** and $[2_2]$-(1,2,4,5)cyclophane **15** (Scheme I),[29] the latter being formed by an apparent [4 + 4] intramolecular "dimerization".

Although it is true that in low-temperature matrices, *o*-quinodimethane itself prefers to dimerize in a [4 + 2] fashion to produce a spiro dimer which predominates over the [4 + 4] adduct by at least 9:1,[29-31] the corresponding intramolecular [4 + 2] "dimer" from **7** would be highly strained and the formation of the [4 + 4] product **15** under gas-phase conditions, therefore, is not surprising. Under the conditions of TMB polymerization in softened matrices or in fluid solution, however, it is likely that the double *o*-quinodimethane **7** may dimerize *intermolecularly* by the [4 + 2] route to give the spiro product **16** (Scheme II).

Attempts to intercept either TMB or its dimers by annealing purple matrices containing the trapping agents dimethyl maleate or fumaronitrile failed to yield any characterizable adducts. Further trapping studies, carried out in fluid media, are described below.

Photochemistry of 1,2,4,5-Tetramethylenebenzene. Photolysis of a frozen solution of ketone **5a** in 2-MTHF with the 313-nm line of a 1000-W lamp generated the characteristic UV–vis spectrum of TMB. Further irradiation at this wavelength did not cause photobleaching of the sample. Irradiation of TMB at its main absorption maximum of 490 nm also was ineffective, although this may have been a consequence of the relatively low output of the Hg–Xe lamp at this wavelength. When the sample was irradiated at 254 nm, however, all of the TMB UV–vis bands decreased in intensity and a new species with absorption maxima at 380 and 410 nm grew in (Figure 7). It was possible to continue photolysis by 254-nm irradiation until >99% destruction of the 490-nm TMB band occurred. Under these conditions, the intensity of the new bands in the 380–410-nm region also diminished, although some residual absorption there could be seen, even after 2 h of irradiation (Figure 7).

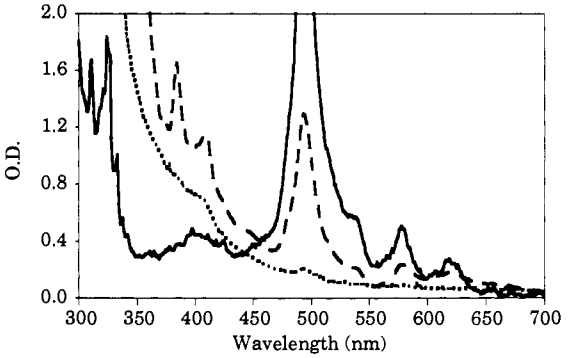

Figure 7. Plot demonstrating the successive photobleaching of TMB **4a** to cyclobuta-*o*-quinodimethane (**18**) and to benzo[1,2:4,5]dicyclobutene (**17**): (—) TMB prior to irradiation, (– – –) after 30 min of 254-nm irradiation, (• • •) after 2 h of 254-nm irradiation.

Scheme III

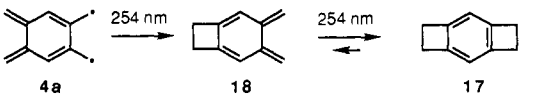

When the matrix was annealed, some polymerization occurred and the presence of the tricyclic hydrocarbon benzo[1,2:4,5]dicyclobutene (**17**) (Scheme III) was inferred by GC/MS analytical comparison with an authentic sample.[32] Roth and co-workers[16] also have reported this photobleaching reaction and interpreted it as sequential ring closures **4a** → **18** → **17**.

The residual absorption in the 380–410-nm region after prolonged irradiation suggested that 254-nm light may establish a photostationary state between the bicyclic and tricyclic hydrocarbons **18** and **17**. This hypothesis was verified by photolysis of a 2-MTHF glass initially containing only tricycle **17**. After 2 h of 254-nm irradiation, the UV–vis spectrum of the photolysate showed bands extending out to 420 nm with a discernible maximum at 380 nm (Figure 8).

In fact, the absorption profile was similar to that observed after prolonged photolysis of TMB itself (Figure 7, 2-h trace). Further irradiation, however, did not increase the optical density at 380 nm nor was there ever any hint of absorption at the TMB characteristic wavelength of 490 nm. This preference for ring closure (**18** → **17**) over ring opening (**18** → **4a**) leaves little hope that photolysis of **17** might produce TMB **4a** directly. Similarly, irradiation of 3,4-cyclobutathiophene does not lead to 3,4-dimethylenethiophene.[33] It may be that the production of non-Kekulé species from cyclobutenes requires excitation to a higher electronic state than is available with conventional photolysis.[34]

Reactions of 7-Oxa[2.2.1]hericene (5a) and TMB (4a) in Fluid solution. The aim of these experiments was to elucidate the reactivity and spin of TMB by generating it from the ketone precursor **5a** and intercepting it with various trapping agents. Results of similar efforts had been reported in publications by Roth and co-workers.[16,17] Thus, heating **5a** at 80 °C in the presence of diethyl fumarate gave compound **19E** (stereochemistry unspecified), which was interpreted as an interception product of the TMB biradical, hypothetically formed by thermal decarbonylation of **5a** (Scheme IV).[16] We, too, obtained a product (79% isolated yield) with the structure of **19E** under such conditions (80 °C, benzene solution, 10 equiv of diethyl fuma-

(29) (a) Boekelheide, V.; Ewing, G. *Tetrahedron Lett.* **1978**, *44*, 4245. (b) Sekine, Y.; Boekelheide, V. *J. Am. Chem. Soc.* **1981**, *103*, 1777.
(30) Errede, L. A. *J. Am. Chem. Soc.* **1961**, *83*, 949.
(31) Trahanovsky, W. S.; Macias, J. R. *J. Am. Chem. Soc.* **1986**, *108*, 6820.
(32) Cava, M. P.; Deana, A. A.; Muth, K. *J. Am. Chem. Soc.* **1960**, *82*, 2524.
(33) Greenberg, M. M. Ph.D. Dissertation, Yale University, 1988; p 76.
(34) Evidence that higher excited states are involved in some photodecyclizations leading to ordinary Kekulé systems is given by the following: (a) Meinwald, J.; Samuelson, G. E.; Ikeda, M. *J. Am. Chem. Soc.* **1970**, *92*, 7604. (b) Labrum, J. M.; Kolc, J.; Michl, J. *J. Am. Chem. Soc.* **1974**, *96*, 2636. (c) Castellan, A.; Kolc, J.; Michl, J. *J. Am. Chem. Soc.* **1978**, *100*, 6687.

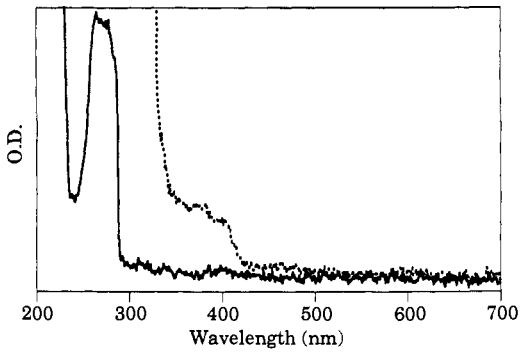

Figure 8. UV–vis spectrum of benzo[1,2:4,5]dicyclobutene (**17**) in 2-MTHF at 77 K: (—) prior to photolysis, (· · ·) after 2 h of 254-nm irradiation.

Scheme IV[a]

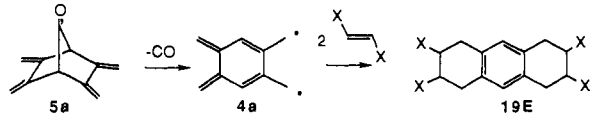

[a] X = CO_2Et.

Scheme V[a]

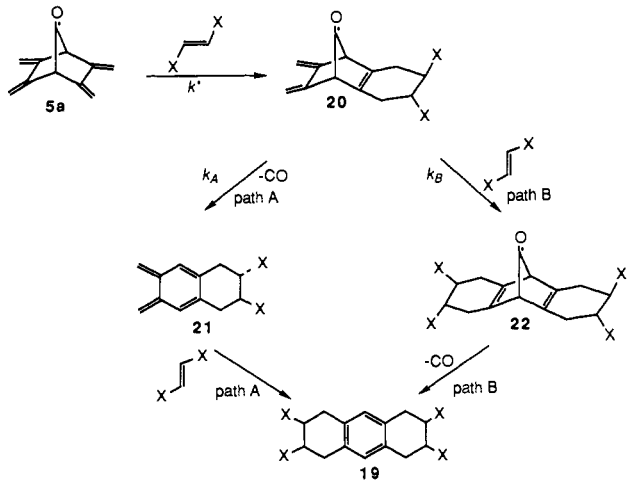

[a] E, X = CO_2Et; CN; X = CN.

rate).[35] However, we found that it is not formed by the decarbonylation-then-addition mechanism proposed[16] in Scheme IV but rather by one of two variants of an addition-then-decarbonylation mechanism (Scheme V), in which biradical **4a** is not an intermediate.

A Diels–Alder addition of diethyl fumarate to one of the conjugated diene units of the intact ketone **5a** initiates the mechanism of Scheme V. The intermediate adduct **20E** now would have two choices. By path A, it could decarbonylate to give the very reactive *o*-quinodimethane **21E**, which then could undergo another Diels–Alder reaction to give **19E**; by path B, the conjugated diene unit of **20E** could undergo a Diels–Alder reaction to give the bis-adduct **22E**, a norbornadienone, which should rapidly decarbonylate to give **19E**. In fact, Rubello and Vogel had already found evidence for the operation of a mechanism initiated by Diels–Alder addition, like that of Scheme V, in the formation of an octahydroanthracene adduct analogous to **19E** in the reaction of ketone **5a** with tetracyanoethylene (TCNE).[19] This reaction occurs at room temperature, where ketone **5a** is

(35) Although two stereoisomers of **19** that preserve the original trans diester configuration of the diethyl fumarate are possible, our material behaved as a single species by the criteria of thin-layer chromatography and both ^1H and ^{13}C NMR spectroscopy. Because the stereodifferentiating sites are remote from each other, it is conceivable that both isomers are present but do not differ detectably in the tests we applied.

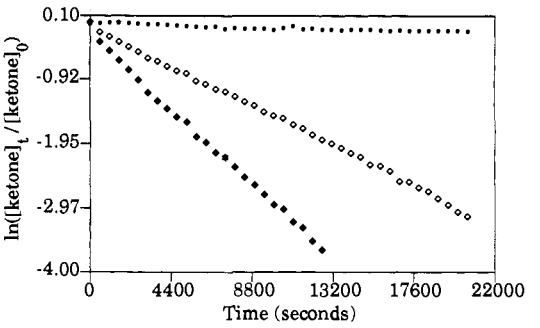

Figure 9. Pseudo-first-order disappearance of ketone **5a** (0.035 M in CD_3CN) at 60 °C in the presence of 0 M (●), 0.5 M (◇), and 1.0 M (◆), diethyl fumarate.

thermally stable. Whether it applies to the case of the much less reactive dienophile diethyl fumarate now becomes an important issue.

A kinetic test provides a straightforward means of distinction between the mechanisms of Schemes IV and V. Scheme IV implies a unimolecular rate-determining step, the decarbonylation of ketone **5a** to biradical **4a**, which should be independent of the concentration of the trapping agent; Scheme V implies a bimolecular rate-determining step, whose rate should be linear in the concentration of the trapping agent. Under pseudo-first-order conditions, if the mechanism of Scheme V prevails, doubling the dienophile concentration should double the rate.

The kinetics of pseudo-first-order decay of ketone **5a** (0.035 M initial concentration in CD_3CN solution) were monitored by ^1H NMR at 60 °C without added trapping agent and also in the presence of 0.5 or 1.0 M diethyl fumarate. Figure 9 shows the results. The ketone alone is essentially unreactive, but it reacts with diethyl fumarate at a rate proportional to the concentration of the trapping agent: $k_{obs} \times 10^4$ s = <0.2, 1.44, and 2.72 for the three fumarate concentrations ($t_{1/2}$ = >500, 80.2, and 42.5 min, respectively).

During the course of the thermal reaction of **5a** with diethyl fumarate, the NMR spectrum showed that peaks associated with a reaction intermediate grew in and then decayed, to be replaced by the peaks associated with the final bis-adduct **19E**. The spectrum of the transient was consistent with structure **20E**, the initial Diels–Alder adduct of Scheme V. No further attempt to isolate **20E** was made, although we did later isolate and characterize by ^1H NMR the corresponding monoadduct **20CN** between **5a** and fumaronitrile. The bis-adduct **19CN** was formed in 72% isolated yield when the thermal reaction of **5a** and fumaronitrile was allowed to proceed to completion. These observations, in conjunction with the kinetic data, leave no doubt that the mechanism initiated by addition (Scheme V) dominates.

The remaining question on the mechanism of Scheme V is which of the two pathways from **20** to **19** does the reaction follow. For reasons given elsewhere,[20] we favor the decarbonylation route (path A) as the more probable one on analogical grounds. The argument depends upon the use of model compounds to estimate the relative rates of the decarbonylation step of path A and of the Diels–Alder first step of path B, the reactions that determine the distribution of material through the competing channels.

The major conclusion from the present experimental data on the *thermal* reactions of the ketone precursor **4a** is that, in contrast to the previous proposal,[16] biradical **5a** is not an intermediate in the formation of the product **19**. The results illustrate once more[36,37] that the occurrence of a reactive intermediate cannot be proven by the nature of the product alone and must be independently demonstrated.

Capture of Photochemically Generated Biradical 4a by Alkenes. Capture of thermally generated biradical **4a** in solution thus is

(36) For kinetic demonstrations of the occurrence of reactive biradical intermediates, see: Reference 37.

(37) (a) Mazur, M. R.; Berson, J. A. *J. Am. Chem. Soc.* **1981**, *103*, 6687. (b) *J. Am. Chem. Soc.* **1982**, *104*, 2217.

Table II. Effect of Concentration on Product Distribution in the Reaction of Fumaronitrile with Photochemically Generated TMB[a]

[5a]	[fumaronitrile]	19CN (mol %)	23CN (mol %)	total yield (%)
0.02	0.1	0	100	70
0.02	1.0	84	16	75

[a] Photolyses (300 nm) were conducted at 0 °C in $CDCl_3$. Product ratios were determined by ^1H NMR in DMSO-d_6.

Scheme VI[a]

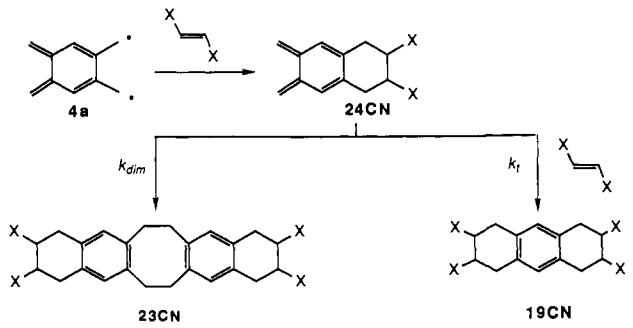

[a] E, X = CO_2Et; CN, X = CN.

not practical because of the competing addition of the trapping agent to the precursor ketone **5a**. To avoid this difficulty, we explored a photochemical route to **4a**. Roth and co-workers had reported that fumaric ester trapped photochemically generated **4a**[16] but also that, under presumably different conditions, it did not.[17] As we shall detail below, the photolysis of ketone **5a** in the presence of alkene trapping agents does, in fact, lead to formal adducts of biradical **4a**.

To establish that the mechanism passes through a reactive intermediate and is not simply a reaction of an excited state of **5a**, we examined the effect of varying trapping agent (fumaronitrile or diethyl fumarate) concentrations on the rate of consumption of **5a** under constant conditions of illumination. Although the data of these studies (see the supplementary material) suffer from some scatter, at least in part because of the accumulation of insoluble material during the runs, the overall results leave little doubt that the rate of disappearance of **5a** is independent of the concentration of trapping agent. This is consistent with the formation of a reactive intermediate by unimolecular photolysis of **5a**.

The product of the photolysis in the presence of diethyl fumarate was difficult to identify. It showed four broad ^1H NMR peaks with chemical shifts appropriate for the 2:2 adduct **23E** (Scheme VI), but the broadness of the peaks made integration difficult, and the material did not return satisfactory ^{13}C or mass spectroscopic data. Significantly, we could find no evidence of the presence of the 2:1 adduct **19E**, which we had previously observed as the only identifiable product in the thermal **5a**–diethyl fumarate reaction.

Photolysis of **5a** in the presence of fumaronitrile gave more useful results. Both the 2:1 (**19CN**) and 2:2 (**23CN**) adducts were formed in relative amounts that depended on the concentration of fumaronitrile (Table II). These observations suggest two candidate mechanisms (Schemes VI and VII).

Scheme VI proposes that the TMB biradical **4a** is captured by fumaronitrile to give *o*-quinodimethane **24CN**, which then can give the 2:2 adduct **23CN** by [4 + 4] cyclodimerization or can add another molecule of fumaronitrile by Diels–Alder addition, to give the 2:1 adduct **19CN**. This proposal seems unlikely because *o*-quinodimethanes prefer to dimerize in a [4 + 2] mode[30] and none of the spiro dimers expected from such a reaction are observed here. Moreover, the laser flash kinetics, to be described below, indicate that dimerization of **4a** in solution is competitive with its capture by alkenes, which suggests an alternative to Scheme VI, shown in Scheme VII.

Scheme VII

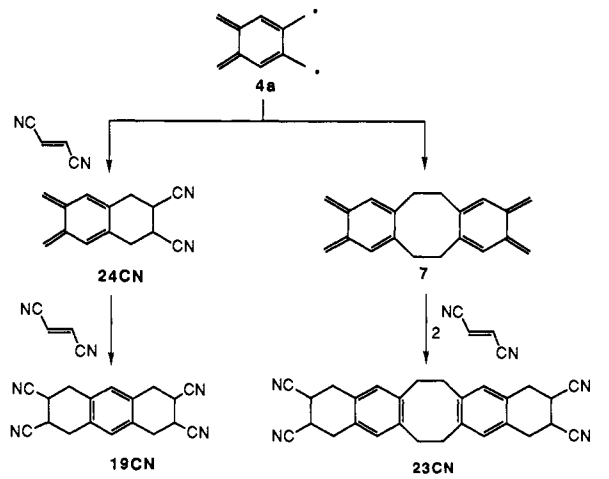

Scheme VIII[a]

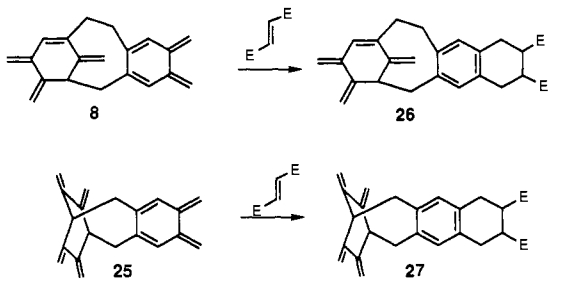

[a] E = CO_2Et.

Scheme VII shows that at sufficiently high alkene concentration, biradical **4a** could be captured by fumaronitrile to give successively **24CN** and **19CN** but at low concentration of alkene, **4a** would dimerize to *bis*(*o*-quinodimethane) **7**, which ultimately would be captured as **23CN** by Diels–Alder additions to each of the two *o*-quinodimethane units. Spectroscopic evidence, to be described below, supports the structure of **7** for the dimer of biradical **4a** observed under the laser flash photolysis conditions. These facts lead us to favor Scheme VII as the correct description of the chemistry of photochemically generated biradical **4a**. Similar results were observed with maleic anhydride as the trapping agent, although the high reactivity[38–41] of that substance permitted the isolation of the 2:1 adduct even at a low (0.16 M) initial concentration of alkene. Mass spectrometry provided presumptive evidence of the presence of the 2:2 adduct in the insoluble portion of the reaction mixture in the maleic anhydride system.

The isolation of a 70% yield of the 2:2 adduct **23CN** (see Table II) means that the dimerization of biradical **4a** occurs predominantly by the symmetrical [4 + 4] pathway (Scheme VII). We considered the possibility that other dimers, for example, **8** and **25** (Scheme VIII), might be formed in smaller amounts but that their Diels–Alder adducts with fumaronitrile might remain entrained in the insoluble material formed in the reaction. However, in the diethyl fumarate trapping experiments, the reaction mixtures remained homogeneous throughout. Furthermore, the NMR spectra of the crude products still showed no evidence of the olefinic absorptions that would be expected from the corresponding Diels–Alder adducts **26** and **27**.

Capture of Photochemically Generated Biradical 4a by Oxygen. Photolysis of an oxygen-saturated $CHCl_3$ solution of oxahericene

(38) (a) Greenberg, M. M.; Blackstock, S. C.; Berson, J. A. *Tetrahedron Lett.* **1987**, *28*, 4263.
(39) Haider, K. W.; Clites, J. A.; Berson, J. A. *Tetrahedron Lett.* **1991**, *32*, 5305.
(40) Scaiano, J. C.; Wintgens, V.; Bedell, A.; Berson, J. A. *J. Am. Chem. Soc.* **1988**, 110, 4050.
(41) Scaiano, J. C.; Wintgens, V.; Haider, K.; Berson, J. A. *J. Am. Chem. Soc.* **1989**, *111*, 8732.

5a at 0 °C gave peroxides **28** and **29** in 30% and 55% yield, respectively. The latter compound also had been reported by

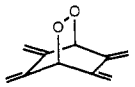

28

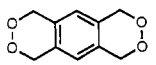

29

Birbaum and Vogel[42] as a product of the photooxidation of [2.2.2]hericene. Roth and co-workers[16,17] also had reported the formation of peroxides **28** and **29** in reactions of the ketone precursor **5a**. The latter authors interpreted this result as evidence in favor of a triplet state of **4a** reacting in a multiplicity-specific sense with O_2. Roth and Scholz[43] also had used a similar argument to explain the trapping reactions of 2,3-dimethylenecyclohexane-1,4-diyl, which reacted with butadiene and with O_2. They attributed the butadiene reaction to the singlet biradical and the oxygen reaction to the triplet, deriving from this reasoning a triplet–singlet gap of 5 kcal/mol. However, the assumption[43] that butadiene reacts only with the singlet state is questionable, since Bauld and Chang[44] had shown that *trans*-penta-1,3-diene reacted with the same biradical, 2,3-dimethylenecyclohexane-1,4-diyl, to give an adduct in which the original diene stereochemistry was not preserved, a result consistent with trapping of the triplet state of the biradical. The triplet states of biradicals in the trimethylenemethane series also react readily with conjugated dienes.[45] Moreover, the assumption[43] that singlet species do not react readily with O_2 is contradicted by a growing body of evidence[46-51] including recent nanosecond time-resolved spectroscopic determinations[51] of the absolute rate constants of O_2 trapping of a series of singlet biradicals, which are in the range of 10^6–10^9 M^{-1} s^{-1}.

The Spin State of 1,2,4,5-Tetramethylenebenzene. Electron Spin Resonance (ESR) Evidence. Photolysis of the oxahericene precursor **5a** in an adamantane matrix has been reported[16] to give rise to an ESR spectrum observed at 15 K in an adamantane matrix and assigned to the triplet state of TMB. The $\Delta m_s = 1$ transition consisted of a narrow signal (total width ~ 90 G) with discernible fine structure which was interpreted with the zero-field splitting parameters $|D/hc| = 0.0042$ cm^{-1} and $|E/hc| = 0.0009$ cm^{-1}. A very weak resonance appeared at approximately half-field, which was assigned to the $\Delta m_s = 2$ transition. The intensity of the ESR signal was linear in $1/T$, which led the authors[16] to assign the ground state of TMB as triplet. Presumably, the Curie law plot measured the signal intensity of the $\Delta m_s = 1$ transition, since the $\Delta m_s = 2$ transition usually is not detected at higher temperatures. Implicit in the authors' interpretation is the assumption that the carrier of the visible color and the UV–vis spectrum is the same species that is responsible for the ESR signal.

The assignment[16] of a triplet ground state to TMB, in contradiction to the computational predictions[13-15] of a substantial preference for the singlet, of course creates a sharp conflict between theory and experiment. However, this is not the only cause of uneasiness. In particular, the value of the reported[16] zero-field splitting parameter, $|D/hc| = 0.0042$ cm^{-1}, seems too small for a biradical species with the structure of **4a**. Application of the point–dipole approximation of the spin dipolar interaction to semiempirical wave functions leads to calculated[52] $|D/hc|$ values of 10 non-Kekulé triplet ground-state biradicals which are consistently larger than the observed values by an average factor of 2.11 ± 0.2 (Table III). It is therefore disturbing that the value of $|D/hc| = 0.0348$ cm^{-1} we calculated for TMB **4a** by this method exceeds the observed[16] one by a factor of 8.29 (Table III).

Table III. Calculated and Experimental Values of the ZFS Parameter $|D/hc|$ for Several Biradicals

biradical	calcd (cm^{-1})	expt (cm^{-1})	calcd/expt
	0.0520	0.0248[a]	2.08
	0.0496–0.0514	0.0250[b]	1.98–2.06
	0.0500	0.0204[c]	2.46
	0.032–0.034	0.012,[d] 0.011[e]	2.66–2.82
	0.0542–0.0568	0.0266[f]	2.04–2.14
	0.0348	0.0042[g]	8.29

[a] Dowd, P. *J. Am. Chem. Soc.* **1966**, *88*, 2587. [b] Reference 12. [c] Roth, W. R.; Erker, G. *Angew. Chem., Int. Ed. Engl.* **1973**, *12*, 503. [d] Wright, B. B.; Platz, M. S. *J. Am. Chem. Soc.* **1983**, *105*, 628. [e] Goodman, J. L.; Berson, J. A. *J. Am. Chem. Soc.* **1985**, *107*, 5409. [f] Rule, M.; Matlin, A. R.; Dougherty, D. A.; Hilinski, E.; Berson, J. A. *J. Am. Chem. Soc.* **1979**, *101*, 5098. [g] Reference 16.

In further study of this issue, we also have now observed ESR spectra by irradiation at 77 K of glassy frozen solutions of the ketone precursor **5a** in 2-MTHF, methylcyclohexane, and diethyl ether and from the cosublimate of **5a** with adamantane. These preparations all produced the same narrow signal in the $\Delta m_s = 1$ region (3280 G at a microwave frequency of 9.27 GHz), whose spectral width was comparable to that reported.[16] We noted, however, that the intensity of the ESR signal was not correlated with the optical density of the UV–vis signal and the purple color. In fact, ESR spectra very similar to those observed in the freshly irradiated purple preparations were readily observed in *colorless* samples that had been prepared by thawing a purple sample and then refreezing and rephotolyzing it.

These observations strongly suggested that the carriers of the UV–vis and ESR spectra were not the same species. Further experiments in the cryogenic temperature region permitted the direct observation of the weak $\Delta m_s = 2$ signal and confirmed this implication. An intensely purple glassy sample, prepared by irradiation at 313 nm of **5a** at 77 K, showed the characteristic strong peak at 490 nm. When cooled to 10 K, this sample showed not only the strong $\Delta m_s = 1$ ESR signal but also the very weak $\Delta m_s = 2$ transition (at 1650 G and 9.295 GHz, Figure 10).

The sample was then photolyzed at 77 K with the unfiltered output of the 1000-W Hg–Xe lamp. As described above, this treatment bleached the purple color. UV–vis inspection of the sample in several regions of the glass showed that all (>99%) of the 490-nm absorption was gone, but reexamination of the bleached sample by ESR at 10 K revealed that the $\Delta m_s = 2$ transition *was still present in undiminished intensity* (Figure 11). In addition, the main ($\Delta m_s = 1$) transition was much stronger, and its fine structure was lost. Thus, the main transition apparently can have a significant amount of doublet contribution. This last observation is also relevant to the reported[16] temperature dependence of the signal intensity of the main ESR band. A substantial doublet component to this band would bias a Curie law plot toward linearity. Accordingly, the reported[16] linearity of the Curie law plot cannot be decisive in this case.

(42) Birbaum, J.-L.; Vogel, P. *Helv. Chim. Acta* **1986**, *69*, 761.
(43) Roth, W. R.; Scholz, B. P. *Chem. Ber.* **1982**, *116*, 1197.
(44) Bauld, N. L.; Chang, C.-S. *J. Am. Chem. Soc.* **1972**, *94*, 7594.
(45) (a) Siemionko, R.; Shaw, A.; O'Connell, G; Little, R. D.; Carpenter, B. K.; Shen, L.; Berson, J. A. *Tetrahedron Lett.* **1978**, 3529. (b) Siemionko, R. K.; Berson, J. A. *J. Am. Chem. Soc.* **1980**, *102*, 3870. (c) Platz, M. S.; Berson, J. A. *Ibid.* **1976**, *98*, 6743. (d) Platz, M. S.; Berson, J. A. *Ibid.* **1980**, *102*, 2358.
(46) (a) Sander, W. *Angew. Chem., Int. Ed. Engl.* **1990**, *29*, 344. (b) Ganzer, G. A.; Sheridan, R. S.; Liu, M. T. H. *J. Am. Chem. Soc.* **1986**, *108*, 1517. (c) Sander, W. W. *Spectrochim. Acta, Part A* **1987**, *43A*, 637.
(47) Adam, W.; Platsch, H.; Wirz, J. *J. Am. Chem. Soc.* **1989**, *111*, 6896.
(48) Burnett, M. N.; Boothe, R.; Clarke, E.; Gisin, M.; Hassaneen, H. M.; Pagni, R. M.; Persy, G.; Smith, R. J.; Wirz, J. *J. Am. Chem. Soc.* **1988**, *110*, 2527.
(49) Lutz, H.; Breheret, E.; Lindqvist, L. *J. Chem. Soc., Faraday Trans. 1* **1973**, *69*, 2096.
(50) Wilson, R. M. In *Organic Photochemistry*; Padwa, A., Ed.; Marcel Dekker: New York, 1985; Vol. 7.
(51) Heath, R.; Bush, L. C.; Feng, X. W.; Berson, J. A.; Berinstain, A.; Scaiano, J. C., submitted for publication.
(52) Rule, M.; Matlin, A. R.; Seeger, D. E.; Hilinski, E. F.; Dougherty, D. A.; Berson, J. A. *Tetrahedron* **1982**, *38*, 787 and references cited therein.

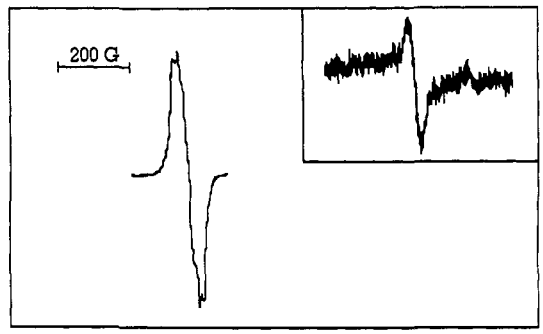

Figure 10. ESR signal observed at 10 K following 313-nm photolysis of ketone **5a** in 2-MTHF. Inset: half-field transition at 1650 G (microwave power = 1 mW).

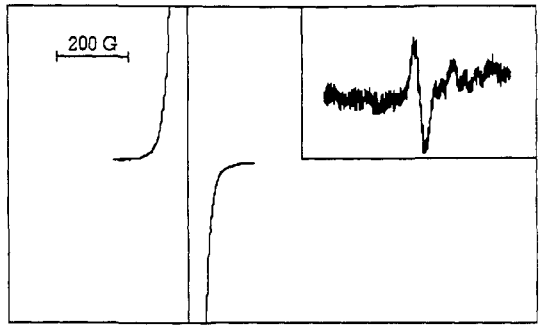

Figure 11. ESR spectrum observed at 10 K following complete (>99%) photobleaching (254 nm) of the 490-nm transient. Inset: half-field transition is still observable. The spectrometer settings are the same as in Figure 10.

The present observations permit the conclusions that *at least two* ESR-active species are generated in these photolyses and that the *UV-vis spectrum is not associated with any of the observed ESR signals*. Moreover, the calculated $|D/hc|$ value of 0.0348 cm^{-1} for triplet **4a** can be divided by the empirical correction factor 2.11 (see above) to give a prediction of $|D/hc| \simeq 0.017$ cm^{-1} for the actual splitting parameter, which would correspond to a total $\Delta m_s = 1$ spectral line width of 360 G. This resonance, approximately four times the width of the observed spectrum, should have been readily visible. We conclude, therefore, that not only is the narrow signal observed not associated with TMB but that it also is unlikely that any appreciable quantity of authentic TMB triplet is present in our ESR preparations. There remains the question of what species is the cause of the triplet ESR spectra. The narrow splitting would be consistent with the weak dipolar interaction of a well-defined radical pair, either intermolecular or intramolecular, but for the present, we can only speculate on this issue.

Identification of the Purple Transient as a Singlet Species by Correlation of UV–Vis and NMR Spectroscopy. Application of cross-polarization magic angle spinning (CP MAS) solid-state ^{13}C NMR spectroscopy has permitted the assignment[53] of singlet states to the matrix-immobilized transient species 3,4-dimethylenefuran (**30**) and 3,4-dimethylenethiophene (**31**).

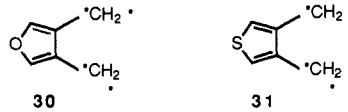

30 31

The basic rationale of these experiments is that the NMR resonances of a triplet biradical should be broadened and Fermi contact-shifted so severely as to be indetectable in the normal ^{13}C NMR region. Accordingly, the appearance of unbroadened bands with normal chemical shifts in the ^{13}C spectra of the two *3,4-dimethylidene-^{13}C* isotopically enriched heterocyclic biradicals establishes the singlet nature of these molecules. ESR is of limited use in the study of singlets, since the necessary property of ESR silence results only in a negative experiment. Therefore, NMR spectroscopy which can provide direct confirmation of singlet character is complementary to ESR in this field.

The principal limitation of the current version of the NMR technique is the need for isotopic enrichment of the transient in order to furnish sufficient signal-to-noise ratio in the CP MAS experiment. For a fair test of singlet character, the enrichment should be at positions of large spin density to maximize any broadening or contact shifting.

We synthesized the labeled oxahericene precursor **5b** from tetraester **6b** by the same method used in the unlabeled series, except that 99% isotopically pure ^{13}CO was used instead of natural abundance CO in the carbonylation step. The solution-phase ^{13}C NMR spectrum of this compound had a single resonance at 105 ppm. In the cases of the ^{13}C-labeled 3,4-dimethylenefuran and 3,4-dimethylenethiophene, the ^{13}C NMR chemical shifts of biradicals **30** and **31**, 102 and 105 ppm, respectively, were well removed from those of the corresponding diazene precursors (59 and 66 ppm) because of the change in hybridization of the labeled carbons from sp^3 to sp^2. No such rehybridization occurs in the transformation **5b** → **4b**, and we were concerned that the resonance of singlet **4b** might unluckily fall directly under that of precursor **5b** and hence be difficult to detect. This would be of special concern in the CP MAS experiment, which gives broader lines than those observed in solution. In this regard, we were encouraged by the previously recorded success[53c] of CP MAS NMR in resolving the resonance of 3,4-dimethylenethiophene-*2,5-di-^{13}C* (115 ppm) from that of its diazene precursor (120 ppm). On the other hand, the spectrum of alcohol **32** showed only one resonance under these conditions, whereas in solution, two peaks at 104 and 106 ppm were visible. This was a warning that the resolving power of the solid state method might be limited to >2 ppm in glassy media.

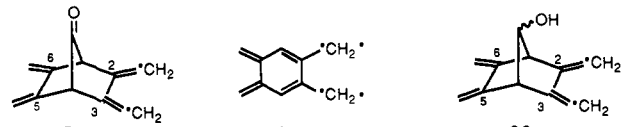

5 4 32

a: •CH_2 unlabeled
b: •CH_2 ^{13}C labeled

Irradiated purple samples of **5b** (0.09–0.11 M) in frozen glassy MTHF (77 K) showed a single new absorption at 113 ppm (Figure 12A) about 8 ppm downfield from that of the precursor (Figure 12B). The growth of this new resonance matched quantitatively (≥95%) the decrease in intensity of the precursor peak at 105 ppm and indicated that the extent of conversion in replicate runs was 38 ± 8%. When the sample was thawed at 120 K, the purple color disappeared and subsequent reexamination of the sample by ^{13}C CP MAS NMR at 77 K showed that the signal also had vanished (Figure 12C).

Similar results were obtained in toluene glasses, where the ^{13}C NMR resonances of the solvent did not obscure the upfield region. The resonance of the transient **4b** appeared again at 113 ppm. The difference spectrum showed that only one new peak was formed in the irradiation of the labeled ketone **5b** and that the decrease in intensity of the ketone methylene resonance at 105 ppm was quantitatively matched by the increase in intensity of the biradical resonance at 113 ppm.

In both media, no other resonances appeared even when the spectroscopic window was opened to 800 ppm. Moreover, the line width of the 113 ppm resonance was normal for a CP MAS spectrum of a glassy sample, as can be seen by comparing it that of the solvent resonances. These results show that the photolysis

(53) (a) Zilm, K. W.; Merrill, R. A.; Greenberg, M. M.; Berson, J. A. *J. Am. Chem. Soc.* **1987**, *109*, 1567. (b) Zilm, K. W.; Merrill, R. A.; Webb, G. G.; Greenberg, M. M.; Berson, J. A. *Ibid.* **1989**, *111*, 1533. (c) Greenberg, M. M.; Blackstock, S. C.; Berson, J. A.; Merrill, R. A.; Duchamp, J. C.; Zilm, K. W. *Ibid.* **1991**, *113*, 2318.

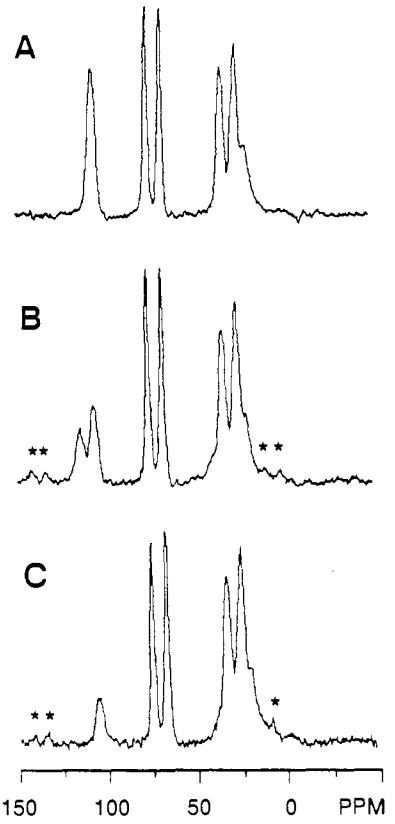

Figure 12. (A) Solid-state CP MAS 13C NMR spectrum of 98% isotopically enriched ketone **5b** in MTHF at 77 K. The four lines between 0 and 80 ppm are MTHF resonances. The line at 105 ppm is the signal of the labeled exocyclic methylene groups of **5b**. (B) Spectrum obtained after irradiation of the above sample at 310 nm at 77 K. The purple color of **4b** is visible. (C) Spectrum obtained by annealing the sample of B to 120 K and then recooling to 77 K. Sample C is colorless. Spinning sidebands in each trace are marked with asterisks.

cleanly converts the precursor **5b** to one species, whose symmetry cannot be lower than that of the precursor ketone **5b** and whose spin state is singlet.

The 113 ppm resonance in the CP MAS spectrum of **4b** remained undiminished in intensity after storage at 77 K for 17 days. Since it cannot be guaranteed that spin equilibrium was achieved during that time, we are reluctant to assign the spin of the ground state. A conservative interpretation of the experiment is that the transient responsible for the NMR spectrum is a *kinetically stable singlet*.

That the NMR spectrum and the purple color disappear together suggests that one species is responsible for both. A more quantitative measure of this correspondence was obtained from a determination of the optical density of the **4b** UV–vis spectrum produced by irradiation of **5b** under conditions identical to those used for the preparation of the above NMR sample. From the extinction coefficient evaluated earlier, the extent of conversion of **5b** to **4b** was 34%, in approximate agreement with the value of 38% determined by NMR.

Structure of the Carrier of the ^{13}C NMR Spectrum. Although the NMR spectrum is readily interpreted in terms of the singlet biradical **4b**, it is necessary to consider whether other structures might also accommodate the data. If the single 113 ppm resonance in the NMR spectrum of the transient simply denotes a symmetry-imposed structural equivalence of the labeled carbons of the NMR-active transient from photolysis of **5b**, the acceptable structures are limited to TMB **4b** and the bicyclic and tricyclic ring-closure products **33** and **17**, respectively. Compound **17** is a known substance.[32] It can be eliminated immediately because the resonance of its CH_2 carbons is at 30 ppm and, in any case, it is a stable compound, not a transient.

Formally, the acyl biradical **34** fails the symmetry test, but it is conceivable that the labeled CH_2 group vicinal to the acyl group might have a chemical shift identical to that of the ketone precursor **5b**. If that were the case, a peak equal in intensity to the 113 ppm peak must have been hidden under the 105 ppm peak of **5b** and the amount of conversion actually would have been twice as large as that calculated on the hypothesis of **4b** as the signal carrier. In the MTHF experiments, the intensity of the 105 ppm peak did diminish noticeably upon annealing the sample (probably because of reaction of **5b** with **4b** or with polymer) but the decrease was not enough to account for the total of >80% apparent conversion. Perhaps an even stronger argument against **34** is the formation of massive amounts of CO in the photolysates of **5a**, as monitored by IR spectroscopy. This argument also would apply if one were to postulate a fortuitous coincidence of the two labeled CH_2 chemical shifts of **34** and attempt to attribute the NMR spectrum solely to that species.

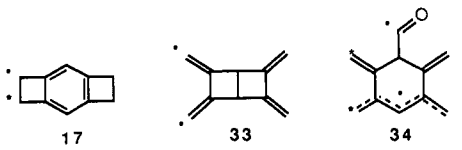

This leaves, as a rival structure to **4b**, only the bicyclic hydrocarbon **33**. This structure is not readily reconciled with the UV–vis spectrum nor with other facts to be presented, but strong arguments against it can be derived from NMR data alone. For example, the chemical shifts of the CH_2 carbons of the model compounds [4]-radialene (**35**) (101.7 ppm)[54] and 1,2-dimethylene-3,4-di-*tert*-butylcyclobutane (**36**) (103.2 ppm)[55] suggest that the resonances of the labeled carbons of **33** should not appear as far downfield as 113 ppm.[56]

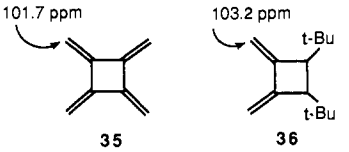

Very recently, Liu, Zhou, and Hinton[59] have provided additional evidence against the bicyclic species **33** as the carrier of the NMR signal. Using the TX-90 program of Pulay, with basis sets 6-31G**, 6-31+G**, and 6-311G**, they calculated the chemical shift shielding tensors for both the ketone precursor **5b** and the hypothetical bicyclic product **33**. They found that, although the actual values of the chemical shifts changed with the basis set used, the *difference* between the shifts of the CH_2 carbons of the precursor ketone **5b** and the hypothetical photoproduct **33** was always less than 1 ppm. Therefore, they proposed that had **33** been formed in the photolysis of **5b**, its NMR resonance would have been indetectable, since it would have fallen directly under that of the precursor. Also, they calculated that the shift of the exocyclic methylene carbon in *o*-quinodimethane (a model[60] of the same type of carbon shift in **4b**) should be at ~6.5 ppm lower field than that of ketone **5b**, in good agreement with our observed shift difference of 8 ppm between ketone **5b** and biradical **4b**. The overall conclusion of Liu and co-workers was that their computational study confirmed the earlier rejection[18a] of **33** we had made on other grounds.

(54) Hopf, H.; Kretschmer, O.; Ernst, L.; Witte, L. *Chem. Ber.* **1991**, *125*, 875.
(55) Trabert, L.; Hopf, H. *Liebigs Ann. Chem.* **1980**, 1786.
(56) The known compounds 2,3-dimethylenebicyclo[2.2.0]hex-5-ene (**35**)[57] and 2,3-dimethylenebicyclo[2.2.0]hexane[58] would also serve as plausible models, but unfortunately, their ^{13}C NMR data are not recorded.
(57) (a) Farr, F. R., Bauld, N. L. *J. Am. Chem. Soc.* **1970**, *92*, 6695. (b) Bauld, N. L.; Farr, F. R.; Chang, C.-S. *Tetrahedron Lett.* **1972**, 2443.
(58) Roth, W. R.; Erker, G. *Angew. Chem., Int. Ed. Engl.* **1973**, *12*, 503.
(59) Liu, R.; Zhou, X.; Hinton, J. *J. Am. Chem. Soc.* **1992**, *114*, 6925.
(60) Although it would have been desirable to compute the chemical shift of biradical **4b** directly, a program for open-shell systems was not available.

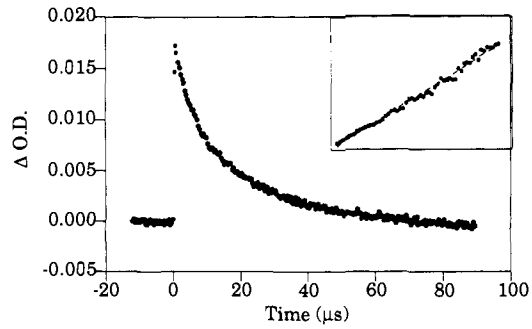

Figure 13. Decay of the 490-nm transient generated by 308-nm laser flash photolysis of ketone **5a** in $CHCl_3$ at 291 K. Inset: second-order fit of the decay data.

Table IV. Dimerization Rates ($2k_t$) and Diffusion Rates (k_{diff}) of the TMB Biradical **4a** in Solution at 291 K

solvent	$2k_t \times 10^{-10}$ M s	viscosity (poise)[a]	$2k_{diff} \times 10^{-10}$ M s
chloroform	2.5 ± 1.3	0.00542	2.4
acetonitrile	3.6 ± 1.8	0.00345	3.8
toluene	1.8 ± 0.9	0.00590	2.2

[a] Values for 20 °C, uncorrected, taken from ref 62.

Absolute Rates of Reaction of the TMB Biradical 4a by Nanosecond Time-Resolved Laser Flash Photolysis. Direct analysis of the kinetics of reactions of biradical **4a** deepens understanding of its properties and provides confirmatory evidence of its structure. When deoxygenated samples of the ketone precursor **5a** in chloroform, toluene, or acetonitrile were subjected to 308-nm laser pulses,[61] the biradical absorption at 490 nm appeared instantaneously on the nanosecond time scale. The maximum optical densities were 0.02–0.05, corresponding to $\sim 1 \times 10^{-5}$ M initial concentrations of the transient. The decay of the 490-nm absorption could be fitted to second-order (but not to first-order) kinetics with correlation coefficients ≥0.99 (Figure 13). Attenuation of the laser dose with neutral density filters showed that the kinetic order and the rate constants were not dependent on the initial transient concentration.

Table IV lists the dimerization rate constants ($2k_t$) calculated from the data using a value for the extinction coefficient of the transient of 5000 M^{-1} cm^{-1} at 490 nm. The flash photolysis experiments also detected the absorptions at 575 and 620 nm. Although the low optical densities at the latter wavelengths resulted in less accurate kinetic fits, the decay traces for the 575-nm absorption gave rate constants within experimental error of those obtained from the 490-nm band. The 620-nm band also declined in parallel fashion, although the signal-to-noise ratio in that case was too low for quantitative determination of a rate constant. Combined with the fluorescence excitation spectra already described, these results clearly point to a single molecular species as the carrier of these three UV–vis absorptions.

The rate constants in Table IV differ slightly from those reported in the preliminary communication,[18b] which used the less accurate value of $\epsilon = 4200$ M^{-1} cm^{-1}. In our opinion, the rate constants are probably reliable to about 50%, the main uncertainty being in the value of the extinction coefficient. The table also lists the rates of diffusion in each of the solvents calculated from the approximate form of the Debye–Stokes–Einstein model: $k_{diff} = 8RT/(3000\eta)$, where η is the viscosity in poise and $R = 8.31 \times 10^7$ erg/mol K.

The rate constants of Table IV, like those observed[40] for 3,4-dimethylenefuran and 3,4-dimethylenethiophene, are close to the limiting ($2k_{diff}$) dimerization rate permitted by the encounter frequency.[63a] For a singlet biradical dimerization, product formation is spin-allowed for all encounters so that no spin-statistical retardation should apply. The experimental error in the rate constants probably is small enough to permit a distinction between singlet dimerization and triplet dimerization, if the statistical factor in the latter reaction is taken to be $^1/_9$, which would be appropriate for a concerted formation of both new bonds. However, if a triplet dimer biradical can be an intermediate on the way to product, the statistical factor would be $^4/_9$. This would give an encounter-limited rate about half that of the singlet dimerization, and the experimental uncertainty of 50% would not permit a reliable distinction between the two. For this reason, we emphasize that the absolute rates of dimerization themselves are not the basis of our assignment of singlet character to the TMB biradical **4a**, which rests upon other criteria given above. Nevertheless, the absolute rates are fully consistent with a singlet carrier of the 490-nm UV–vis absorption. Moreover, they are incompatible with two alternative hypotheses employing the tetramethylene Dewar benzene **33** and therefore provide the basis for their systematic refutation.

Thus, by analogy to 2,3-dimethylenebicyclo[2.2.0]hex-5-ene (**37**), which persists in solution at room temperature for several days,[57] dimerization of **33** would not be expected to occur at the rate observed for the 490-nm transient, which is 10^{15}-fold faster.

37

Similarly untenable is a hypothesis that photolysis of ketone **5a** gives rise to a *mixture* of biradical **4a** and bicyclic hydrocarbon **33**, in which **4a** is responsible for the UV–vis spectrum and **33** is responsible for the NMR spectrum. Because the conversion in the photolysis monitored by NMR is essentially quantitative, no more than about 5% of any species (*e.g.*, **4a**) other than that responsible for the 113-ppm ^{13}C NMR resonance can be present. Thus, the UV–vis-active species would have to be assigned an extinction coefficient ≥20 times that originally determined. This would lead to the unacceptable assignment of rate constants for the dimerization of **4a** in the range $\geq 4 \times 10^{12}$ M^{-1} s^{-1}, or 400 times the encounter-controlled limit.

Structure of the Primary Product of the Dimerization of TMB Biradical 4a. As was observed in the low-temperature matrix experiments, the decay of the biradical absorption at 490 nm is accompanied by the growth of a new absorption maximum at 380 nm.[18b] We assign this to the *o*-quinodimethane **7**, which we previously proposed as the intermediate in the formation of the trapping product **23CN** (Scheme VII) when **4a** is generated in dilute solutions of fumaronitrile. In the flash photolysis experiment, the increase in concentration of the 380-nm species **7** (assumed to have $\epsilon_{380} = 6000$ M^{-1} cm^{-1}, or twice the extinction coefficient of *o*-quinodimethane itself) in a specific time interval (0.3–7.0 μs) is about 78% of the decrease in concentration of the 490-nm transient, which would be compatible with the observed formation of a 70% yield of adduct **23CN** in the fumaronitrile trapping experiment.

The conclusion seems definite that the primary dimerization product of biradical **4a** is bis(*o*-quinodimethane) **7**. This provides compelling confirmatory evidence that the purple carrier of the UV–vis spectrum is not a minor species of undefined structure but rather is one that embodies the TMB unit or one easily convertible to it.

(61) The nanosecond laser system has been described in detail elsewhere. See: Scaiano, J. C. *J. Am. Chem. Soc.* **1980**, *102*, 7747.

(62) *Handbook of Chemistry and Physics*; Weast, R. C., Ed.; CRC Press: Boca Raton, FL, 1987.

(63) (a) For a thorough review of spin-statistical factors in radical–radical reactions, see: Saltiel, J.; Atwater, B. *Adv. Photochem.* **1988**, *14*, 1. (b) The comparison is sensitive to the exact values of the extinction coefficients used in the calculation, and it may also be the case that some oligomerization of **7** takes place under these conditions, which would deplete the amount of **7** detected. In accord with this hypothesis, the growth of the 380-nm absorption was initially second order, but after ~10 μs, the plot of 1/OD vs *t* was no longer linear. In fact, further evidence for a secondary reaction of **7** may be seen in the slight decrease in intensity of the 380-nm band at the longest times studied (33 μs).

Scheme IX[a]

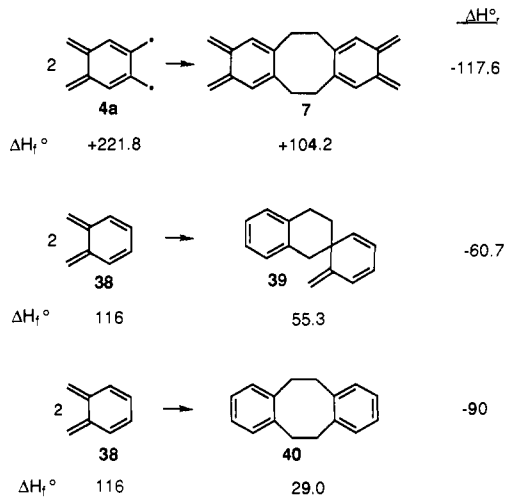

[a] $\Delta H°$ values in kcal/mol.

Comparison of the Dimerization Rate of the TMB Biradical with That of *o*-Quinodimethane. Biradical vs Biradicaloid. The biradicaloid[28,64] hydrocarbon *o*-quinodimethane dimerizes, largely by a [4 + 2] cycloaddition,[29-31] with a rate constant of $\sim 1 \times 10^4$ M^{-1} s^{-1} at 298 K.[31,65] This is to be compared with the rate of dimerization of a true biradical, **4a**, $\sim 1\text{–}3 \times 10^{10}$ M^{-1} s^{-1}, determined in the present work. This observed acceleration of 10^6 actually is a minimum value, since the intrinsic dimerization rate of **4a** may be considerably faster than the diffusive limit. The enhanced reactivity of **4a** probably is the result of a much greater exothermicity in its dimerization and a much smaller HOMO–LUMO energy gap. In Marcus and related rate theories,[66] these factors would be expected to strongly influence the thermodynamic component and the intrinsic barrier height, respectively.

Scheme IX shows the enthalpy changes for the dimerizations of **4a** and *o*-quinodimethane **38**. Heats of formation have been estimated using group equivalents.[67] In the case of **38**, the calculated value closely matches the average of two independent experimental determinations.[65,68] It is clear that even though the predominant dimerization of **38** (which gives **39** in preference to **40**) enjoys the benefit of forming a benzene nucleus, the dimerization of **4a** to the nonbenzenoid species **7** is 57 kcal/mol more exothermic.

π-Biradicaloid hydrocarbons characteristically have small frontier orbital energy gaps,[28,64] and this fact has been invoked to explain the high reactivity of *o*-quinodimethane **38** in cycloadditions.[69] Although the frontier orbital gap is small ($\sim 0.6\beta$ at the level of simple Hückel theory for **38**, for example) compared to that of other formally closed-shell π-conjugated molecules, one should recognize that the gap is still much larger than that for a true non-Kekulé biradical (0.0β for the degenerate HOMO–LUMO pair of **4a** at the simple Hückel level). AM1/CI calculations[70] place the frontier orbital gap at 1.06 eV for **38** and 0.29 eV for **4a**.

The $>10^6$-fold enhancement of the reactivity of biradical **4a** over that of biradicaloid **38** corresponds to a decrease in $\Delta G^{\ddagger}$ of at least 8.2 kcal/mol. It is instructive to think of this decrement as a measure of an energetic consequence of non-Kekulé character.

Attempted Quenching of the TMB Biradical Transient UV–Vis Spectrum with Alkenes. The lifetime of the transient produced in flash photolysis, monitored at the main 490-nm absorption, was independent of the concentration of the diylophilic alkene trapping agents diethyl fumarate (up to 0.40 M), fumaronitrile (0.22 M), or maleic anhydride (0.1 M). The detection limits of the nanosecond photochemical apparatus placed an upper limit of $\sim 10^4$ M^{-1} s^{-1} for the reaction rate with these traps. In a sense, these results were disappointing, since they failed to corroborate the intermediacy of biradical **4a**, which had been implicated in the formation of 2:1 adducts with both fumaronitrile and maleic anhydride in the preparative trapping experiments already described. However, the negative flash photolysis results were consistent with the observations in the preparative trapping that these reactions were slow compared to the dimerization of **4a**.

Trapping competes with dimerization under preparative conditions but not under flash-photolytic conditions, probably because under conditions of laser irradiation, the concentration of the reactive intermediate can easily exceed, by 3 orders of magnitude, those achieved under steady-state photolysis.[71,72] In the present case, the following analysis suggests that the absolute rate constant for reaction of **4a** with alkenes could be as low as 10^2 M^{-1} s^{-1} and still allow trapping to compete with dimerization under the steady-state conditions of the preparative runs. Thus, the initial concentration of **4a** under the laser-flash conditions was $\sim 10^{-5}$ M. If the concentration of **4a** in the steady-state experiments was 1000-fold lower, or 10^{-8} M, then the dimerization rate under the steady-state conditions was roughly $(10^{10}$ M^{-1} $s^{-1})(10^{-8}$ $M)^2$ $= 10^{-6}$ M s^{-1}. Under the same conditions, the rate of trapping in the presence of 1 M alkene, assuming a trapping rate constant of 10^2 M^{-1} s^{-1}, would have been $(10^2$ M^{-1} $s^{-1})(10^{-8}$ M)(1 M), which also is 10^{-6} M s^{-1}, and therefore competitive with the rate of dimerization. This analysis also is consistent with the observation already reported that it was possible to change the reaction product in the preparative runs by changing the concentration of the trapping agent fumaronitrile. High concentrations favored trapping of **4a** itself, and low concentrations favored trapping of **7**, the dimer of **4a** (see Scheme VII).

The reactions of TMB biradical **4a** with alkenes appear to be at least 10^2–10^4 slower than those of 3,4-dimethylenefuran and 3,4-dimethylenethiophene.[40,41] Frontier orbital theory provides a qualitative explanation for the lower reactivity of TMB. Because of through-space interaction, the symmetric component of the nominally nonbonding MOs of TMB is the HOMO but this situation is reversed in the case of the heterocyclic biradicals, where the antisymmetric component is the HOMO (Chart II).[10a,73,74] Phase matching of the biradical HOMO and the antisymmetric alkene LUMO in the cycloaddition transition state can occur with the heterocyclic biradicals but not with TMB.

Absolute Rate of Capture of TMB Biradical 4a by O_2. Under the laser flash conditions, the 490-nm, 575-nm, and 620-nm absorptions of the TMB transient were quenched in O_2- or air-saturated solvents. For the 490-nm band, the quenching showed pseudo-first-order kinetics. Extrapolation of the rate constant vs O_2 concentration data to zero O_2 concentration in chloroform gave a limiting rate constant which, when converted to second-order form, had the value of $\sim 1.0 \times 10^{10}$ M^{-1} s^{-1}, in reasonable agreement with the directly observed dimerization rate constant of $(2.5 \pm 1.3) \times 10^{10}$ M^{-1} s^{-1}. A three-point ($[O_2]$ = 12.0, 2.4, and 0.12 mM) quenching plot of the observed pseudo-first-order rate constant vs $[O_2]$ gave a second-order rate constant for the reaction **4a** + O_2 of 1.85×10^7 M^{-1} s^{-1} in chloroform at 291 K.

(64) Kolc, J.; Michl, J. *J. Am. Chem. Soc.* **1973**, *95*, 7391.
(65) Roth, W. R.; Biermann, M.; Dekker, H.; Jochems, R.; Mosselman, C.; Hermann, H. *Chem. Ber.* **1978**, *111*, 3892.
(66) Murdoch, J. R. *J. Am. Chem. Soc.* **1983**, *105*, 2159 and references cited therein.
(67) Benson, S. W.; Cruickshank, F. R.; Golden, D. M.; Haugen, G. R.; O'Neal, H. E.; Rodgers, A. S.; Shaw, R.; Walsh, R. *Chem. Rev.* **1969**, *69*, 279.
(68) Pollack, S. K.; Raine, B. C.; Hehre, W. J. *J. Am. Chem. Soc.* **1981**, *103*, 6308.
(69) Fleming, I. *Frontier Orbitals and Organic Chemical Reactions*, Wiley-Interscience: New York, 1976.
(70) Blackstock, S. C. Yale University, unpublished results.
(71) For a review, see: Hadel, L. M. In *Handbook of Organic Photochemistry*; Scaiano, J. C., Ed; CRC Press: Boca Raton, FL, 1989; Vol. 1, p 290.
(72) Johnston, L. J.; Scaiano, J. C. *Chem. Rev.* **1989**, *89*, 521.
(73) (a) Du, P.; Hrovat, D. A.; Borden, W. T. *J. Am. Chem. Soc.* **1986**, *108*, 8086.
(74) See also: References 13b and 23.

Chart II

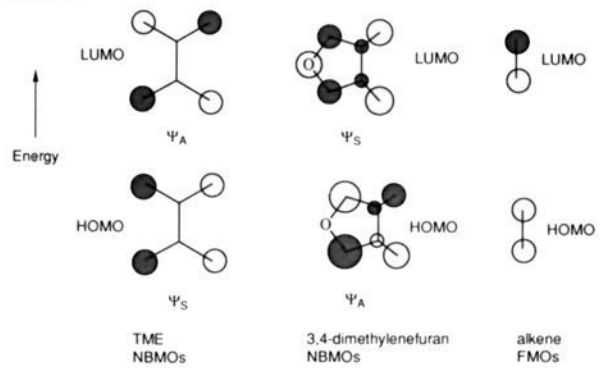

Scheme X

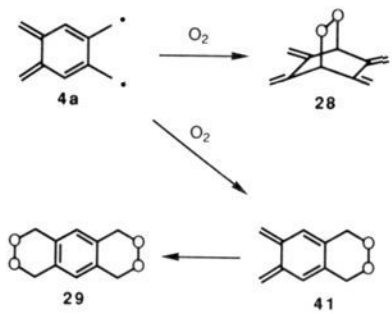

Single-point ([O_2] = 12.0 mM) data for acetonitrile and toluene gave rate constants of (3.1 and 2.2) × 10^7 M^{-1} s^{-1}, respectively.

The disappearance of the 490-nm absorption of **4a** in the time-resolved O_2 quenching experiments was accompanied by the growth of another intermediate which absorbed at 380 nm. The growth of the 380-nm band followed first-order kinetics. A transient absorption spectrum, determined in O_2-saturated chloroform, showed that the new intermediate was relatively stable on the nanosecond time scale. These results are reminiscent of those made during the time-resolved observation of the dimerization of **4a**, in which the *o*-quinodimethane intermediate **7** (Scheme VII) can be detected. Analogously, we assign structure **41** (Scheme X) to the transient, which is the likely intermediate in the formation of diperoxide **29** observed in the preparative trapping experiments with O_2.

According to the mechanism of Scheme X, the product ratio (**29**:**28**) of di- to monoperoxide would be determined by the relative rates of trapping to form the two monoperoxides **41** vs **28**. In the preparative experiments, the product ratio **29**:**28** has the value 1.83 (55:30%), which is close to the 2:1 value that would result from a statistically controlled competition. In the nanosecond experiments, the product **28** is not detectable in our system but the intermediate **41** can be followed by the 380-nm absorption. If the same product ratio of 1.83:1 applies to the competition **41**:**28**, then the concentration of the intermediate **41** should grow until it reaches 0.647 (1.83/2.83) times the initial concentration of the **4a** produced by the laser flash. Experimentally, this initial concentration was 4.1 × 10^{-6} M (on the basis of ϵ_{490} = 5000 M^{-1} cm^{-1}), so that the growth in concentration of **41** should reach 2.65 × 10^{-6} M. Although the extinction coefficient of **41** is not known, it should be close to that of *o*-quinodimethane **38** (3000 M^{-1} cm^{-1}). Combining this assumption with the measured increase of optical density at 380 nm (0.00565) and the optical path length (0.7 cm), we calculated the observed increase in concentration of the intermediate **41** as 2.69 × 10^{-6} M. Given the uncertainties in the extinction coefficients, the agreement with the predicted value probably could not be better. The analysis of the *o*-quinodimethane growth kinetics in these oxygen trapping experiments is on a firmer basis than that in the dimerization study because in the oxygen trapping work, the intermediate **41** did not suffer any secondary decay process on the nanosecond time scale.

The rate of reaction of **4a** with oxygen at 291 K, (1.9–3) × 10^7 M^{-1} s^{-1}, is 3 orders of magnitude less than that of the diffusion-controlled limit and at least 100 times less than the known rates k' of reactions of oxygen with triplet biradicals.[75] Examples include triplet perinaphthadiyl,[76] k' = 2.4 × 10^9 M^{-1} s^{-1}, and the localized biradicals produced by Norrish II photocleavage of ketones,[77] $k' \sim 10^{10}$ M^{-1} s^{-1}. Adam and co-workers[78] have found that the rates of oxygen trapping for several triplet biradicals are well correlated by the equation $k' = (^4/_9)k_{diff}$. By contrast, the literature heretofore has contained few if any measurements of the rates of singlet biradical reactions with O_2, but recent studies[51] of a series of such transients now have shown that for several 3,4-dimethylenepyrrole biradicals as well as for their furan and thiophene counterparts, the rate constants vary between 8.9 × 10^6 and 8.3 × 10^8 M^{-1} s^{-1}, substantially lower than those of triplet biradicals. The evidence strongly suggests that if the TMB biradical **4a** were a triplet species, the rate of its reaction with oxygen should have been near the statistically modified encounter-limited plateau at ~5 × 10^9 M^{-1} s^{-1}.

Similarly, a number of triplet carbenes[79-81] react with oxygen at rates near 5 × 10^9 M^{-1} s^{-1}, but the reactions of singlet carbenes are slower. Thus, phenylchlorocarbene does not react with oxygen on the nanosecond time scale, from which a maximum rate constant of 10^4 M^{-1} s^{-1} is derived,[82a,b] and (*p*-nitrophenyl)chlorocarbene reacts[82c] with a rate constant of 2.24 × 10^7 M^{-1} s^{-1}.

A recent determination of the heat of formation of the TMB biradical **4a**[17] made use of data on the rate of its supposed reaction with O_2 in the gas phase. An important assumption[17] in the analysis of the kinetics was that the reaction of **4a** with O_2 occurs at the statistically modified collision-limited rate. As we have just seen, the rate of the **4a**–O_2 reaction in the solution phase falls short of the encounter frequency by a factor of 10^3, which raises the question of whether the gas-phase reaction may also be correspondingly retarded. If so, a revision of the derived[17] heat of formation of the TMB biradical **4a** would be required.

Summary of Physical Properties of Biradical 4a. Table V collects the physical properties determined in the present work.

Conclusions. The species responsible for the ESR spectrum observed in irradiated low-temperature matrices of 7-oxa[2.2.1]hericene (**5a**) is not the same as the one responsible for the purple color and the UV–vis absorption (λ_{max} = 490, 570, and 620 nm). The latter species is identified as the TMB biradical **4a** by several lines of evidence. In preparative experiments, it can be trapped by alkenes and by oxygen to give bis-adducts embodying the TMB unit. In time-resolved flash photolysis experiments, it is observed to react by trapping or dimerization to give intermediates containing an *o*-quinodimethane unit. In its isotopically enriched form **4b**, its methylene carbons can be

(75) (a) Adam, W.; Grabowski, S.; Wilson, R. M. *Acc. Chem. Res.* **1990**, *23*, 165.
(76) Burnett, M. N.; Boothe, R.; Clarke, E.; Gisin, M.; Hassaneen, H. M.; Pagni, R. M.; Persy, G.; Smith, R. J.; Wirz, J. *J. Am. Chem. Soc.* **1988**, *110*, 2527.
(77) Naito, I. *Bull. Chem. Soc. Jpn.* **1983**, *56*, 2851.
(78) (a) Adam, W.; Hössel, P.; Hümmer, W.; Platsch, H.; Wilson, R. M. *J. Am. Chem. Soc.* **1987**, *109*, 7570. (b) Adam, W.; Grabowski, S.; Wilson, R. M.; Hannemann, K.; Wirz, J. *J. Am. Chem. Soc.* **1987**, *109*, 7572. (c) Adam, W.; Grabowski, S.; Platsch, H.; Hannemann, K.; Wirz, J.; Wilson, R. M. *J. Am. Chem. Soc.* **1989**, *111*, 751.
(79) (a) Werstiuk, N. H.; Casal, H. L.; Scaiano, J. C. *Can. J. Chem.* **1984**, *62*, 2391. (b) Casal, H. L.; Tanner, M.; Werstiuk, N. H.; Scaiano, J. C. *J. Am. Chem. Soc.* **1985**, *107*, 4616. (c) Barcus, R. L.; Hadel, L. M.; Johnston, L. J.; Platz, M. S.; Savino, T. G.; Scaiano, J. C. *J. Am. Chem. Soc.* **1986**, *108*, 3928. (d) Sugawara, T.; Iwamura, H.; Hayashi, H.; Sekiguchi, A.; Ando, W.; Liu, M. T. H. *Chem. Lett.* **1983**, 1261.
(80) Nazran, A. S.; Griller, D. *J. Am. Chem. Soc.* **1984**, *106*, 543.
(81) Sander, W. *Angew. Chem., Int. Ed. Engl.* **1990**, *29*, 344.
(82) (a) Turro, N. J.; Butcher, J. A., Jr.; Moss, R. A.; Guo, W.; Munjal, R.; Fedorynski, M. *J. Am. Chem. Soc.* **1980**, *102*, 7576. (b) Turro, N. J.; Lehr, G. F.; Butcher, J. A., Jr.; Moss, R. A.; Guo, W. *J. Am. Chem. Soc.* **1982**, *104*, 1754. (c) Liu, M. T. H.; Bonneau, R.; Jefford, C. W. *J. Chem. Soc., Chem. Commun.* **1990**, 1482.

Table V. Physical Properties of the TMB Biradical **4a**

property	value
UV–vis[a] (λ_{max})	490 (5000), 530 (sh) (800), 575 (800), 620 (500)
IR[b] (λ_{max})	808, 849
^{13}C NMR of CH_2 (ppm)	113
ESR	none
rate of dimerization[c,d] ($2k_t$)	$(1.9–3) \times 10^{10}$
rate of capture by alkenes[c] (k)	$<10^4$
rate of capture by O_2[c,d] (k)	1.86×10^7

[a] Wavelength in nm (extinction coefficient in M^{-1} cm^{-1}). [b] Frequency in cm^{-1}. [c] Rate constant in M^{-1} s^{-1}. [d] Depends on solvent; 291 K.

directly observed by CP MAS ^{13}C NMR spectroscopy to have a chemical shift of 113 ppm, which is unbroadened and at the proper location for that structural feature. The spin state of the TMB biradical is determined to be singlet by this NMR experiment, which provides an observable property complementary to the absence of an ESR signal. Moreover, the absolute rate of its dimerization is at the encounter-controlled limit, but the rate of its capture by O_2 is slower than that limit by 1000-fold. This behavior again indicates a singlet as the reactive species.

The triplet state of TMB has not yet been observed. The singlet persists for weeks at 77 K and is stable up to the softening point of a poly(methyl methacrylate) matrix at ~200 K. This behavior is consistent with the theoretical prediction of a singlet ground state for this disjoint molecule.

It should be a matter of general concern that spin equilibrium cannot be guaranteed in any system, such as this one, in which only one of the spin isomers has been observed.[83] Accordingly, we refrain from a definite assignment of the ground-state spin. Nevertheless, it is clear that the species previously thought[16,17] to be a triplet is, in fact, a *kinetically stable singlet*. Therefore, there is, at present, no experimental basis for a challenge to theory in the case of TMB. By extension, the disjoint hypothesis must be taken seriously in other cases. The exact theoretical calculation of the ordering and separation of nearly degenerate spin states is still a formidable task,[10,11] and in any given case, a particular level of theory may succeed or fail to identify which one is the more stable. However, this (presumably transitory) computational problem should not obscure the fact that by all present indications, the qualitative disjoint theory is sound in its major claims. Connectivity does profoundly influence the relative energies of spin states of non-Kekulé molecules. Therefore, in disjoint cases, one may properly expect any preference for the triplet to be small or actually inverted.[84]

Experimental Section

General Instruments and Equipment. ^1H NMR spectra were obtained on a Bruker WM-250 (250 MHz) or a Jeol FX 90-Q (90 MHz) spectrometer. Solution-phase ^{13}C NMR spectra were recorded on a Bruker WM-250 (62.5 MHz) spectrometer. Chloroform (δ 7.24), benzene (δ 7.15), deuterium oxide (δ 4.60), methanol (δ 3.75), dimethyl sulfoxide (δ 2.49), acetone (δ 2.15), or acetonitrile (δ 1.93) was used as an internal reference for ^1H NMR. Chloroform (δ 77.7), methanol (δ 59.0), or dimethyl sulfoxide (δ 39.5) was used as an internal reference for ^{13}C NMR. Spectral data are reported as follows: chemical shift, multiplicity, number of protons, and coupling constants (when available). Variable temperature NMR spectra were recorded on the Bruker WM-250 spectrometer using a Bruker VT 1000 Cu–constantan variable temperature controller. Solid-state CP MAS ^{13}C NMR spectra were obtained using an Oxford cryomagnet operating at 25.15 MHz. Hexamethylbenzene was used as an external reference.

Low-resolution mass spectra were obtained using a Hewlett-Packard 5985 GC/MS or a Hewlett-Packard 5890 Series II GC/MS operating at 70 eV. Mass spectral data are reported m/z (relative abundance). High-resolution mass spectra were obtained by Mr. Dan Pentek using a Kratos MS80 RFA spectrometer. Analytical capillary gas chromatography was performed on a Hewlett Packard 5890 gas chromatograph using split–splitless injection and flame-ionization detection. The GC was equipped with a 25-m 5% phenyl–methyl silicone capillary column (0.31-mm i.d. × 0.17-μm film thickness). The retention times of compounds of interest are reported with their spectral data.

Ultraviolet–visible spectra were recorded on a Perkin-Elmer Lambda 6 spectrophotometer equipped with a Digital Equipment Corporation 316sx DEC station for data acquisition and workup. Fluorescence emission–excitation spectra were recorded on a Perkin-Elmer Model 650-40 fluorescence spectrophotometer. Infrared spectra were recorded on a Nicolet 5-SX or a Nicolet 7000 Series FT-IR spectrometer. Cryogenic matrix-isolated UV–vis and IR spectra were obtained using an Air Products closed-cycle helium cryostat (Displex Model CSW-202). Electron spin resonance spectra were recorded on a Varian E-9 EPR spectrometer.

Photolyses were conducted using either a Rayonet photoreactor (Model RPR-100) equipped with 3000-Å lamps, a 200-W high-pressure Hg(Xe) lamp (Oriel 6183), or a 1000-W high-pressure Hg(Xe) lamp (Oriel 6193). Wavelength-selective irradiation was performed with an Oriel 77250 monochromator equipped with an Oriel 77297 grating. A slit width of 2 mm was used, which provided a bandwidth of 10 nm. Longpass irradiation was performed using the appropriate filters where specified.

Laser flash photolysis (LFP) studies used a modification of the system previously described.[85]

Melting points were recorded on a Thomas-Hoover capillary apparatus and are uncorrected.

Solvents and Reagents. Methanol was distilled from Mg/I_2 before use. Tetrahydrofuran (THF) was distilled from sodium and benzophenone under N_2. Diethyl ether, pentane, hexane, and methylene chloride were distilled from CaH_2 under N_2 before use. Dimethyl sulfoxide (DMSO), acetonitrile, benzene, and toluene were distilled from CaH_2 and stored over 3-Å molecular sieves. Pyridine was distilled from BaO and stored over KOH. 2-Methyltetrahydrofuran (2-MTHF) was distilled twice from potassium permanganate and stored over $LiAlH_4$. It was distilled from $LiAlH_4$ immediately prior to use. Unless specified otherwise, reagents were used as received without further purification.

Unless specified elsewhere, all reactions were run under dry nitrogen in glassware that was either flame- or oven-dried. Flash column chromatography was performed on Merck Kieselgel 60 (230–400 mesh). Analytical thin-layer chromatography was performed using Merck TLC plates precoated with Kieselgel 60.

1,2,3,4,5,6,7,8-Octahydroanthracene-2,3,6,7-tetracarboxylic Acid Tetraethyl Ester (19E). A solution of ketone **5a** (20 mg, 0.127 mmol) and diethyl fumarate (220 mg, 1.27 mmol, 10 equiv) in toluene (5 mL) was stirred at 80 °C for 10 h. The volatiles were removed *in vacuo*, and the residue was triturated with pentane/ether (4:1, 5 mL). The white solid was collected by filtration and washed with pentane (2 × 2 mL): yield 45 mg (75%); GC retention time (T_i = 240 °C (isothermal) inj = 250 °C, det = 300 °C) 63.52 min (20.8%), 64.88 min (79.2%); ^1H NMR (250 MHz, $CDCl_3$) δ 6.84 (s, 1H), 4.20 (q, J = 7.1 Hz, 4H), 3.15–2.8 (m, 6H), 1.28 (t, J = 7.1 Hz, 6H); ^{13}C NMR (62.5 MHz, $CDCl_3$) δ 175.07, 132.69, 129.15, 61.47, 42.90, 32.07; FTIR (cm^{-1}) 1726, 1301, 1237, 1185, 1150, 1022; DIP/MS (70 eV) m/z 474 (M^+, 28.9), 429 (25.8), 400 (79.2), 355 (35.1), 354 (34.0), 327 (35.4), 326 (89.7), 281 (48.1), 253 (48.1), 179 (100); exact mass calcd for $C_{26}H_{34}O_8$ 474.2254, found 474.2275.

1,2,3,4,5,6,7,8-Octahydroanthracene-2,3,6,7-tetracarboxylic Dianhydride. A solution of ketone **5a** (20 mg, 0.127 mmol) and maleic anhydride (50 mg, 0.506 mmol, 4 equiv) in $CHCl_3$ (4 mL) was stirred at 25 °C for 24 h. The white precipitate was collected by filtration and washed with diethyl ether (3 × 5 mL): yield 35 mg (85%), white solid; mp >200 °C; ^1H NMR (250 MHz, DMSO-d_6) δ 7.08 (s, 1H), 3.75, 3.65 (2 s, 2H), 3.01–2.85 (m, 4H); ^{13}C NMR (62.5 MHz, DMSO-d_6) δ 174.41, 133.60, 126.54, ~40 (obscured by DMSO), 28.09; FTIR (cm^{-1}) 1836, 1770, 1233, 1191, 1070, 978, 957, 914; DIP/MS (70 eV) m/z 326 (M^+, 67.7), 298 (100), 253 (73.6), 252 (66.2), 181 (55.2), 179 (88.4), 141 (28.2); exact mass calcd for $C_{18}H_{14}O_6$ 326.0790, found 326.0779.

2,3,6,7-Tetracyano-1,2,3,4,5,6,7,8-octahydroanthracene (19CN). A solution of ketone **5a** (20 mg, 0.127 mmol) and fumaronitrile (39 mg, 0.506 mmol) in toluene (5 mL) was stirred at 80 °C for 15 h. The solvent was evaporated, and the residue was taken up with diethyl ether (5 mL). This heterogeneous solution was placed in a 15-mL centrifuge tube, and the solid was spun down to the bottom of the tube. The ether was decanted,

(83) Bush, L. C.; Heath, R. B.; Berson, J. A. *J. Am. Chem. Soc.* In press.
(84) (a) For experimental and theoretical studies of other disjoint systems, see: References 8a and 84b–e. (b) Itoh, K. *Pure Appl. Chem.* **1978**, *50*, 1251. (c) Murata, S.; Sugawara, T.; Iwamura, H. *J. Am. Chem. Soc.* **1987**, *109*, 1266. (d) Murata, S.; Iwamura, H. *J. Am. Chem. Soc.* **1991**, *113*, 5547. (e) For a review, see: Borden, W. T. *Mol. Cryst. Liq. Cryst.*, in press.
(85) Scaiano, J. C. *J. Am. Chem. Soc.* **1980**, *102*, 7747.

and the solid was washed with fresh ether (2 × 5 mL), spinning down after each washing: yield 26 mg (72%), beige powder; mp >200 °C; ^{1}H NMR (250 MHz, DMSO-d_6) δ 6.95 (s, 1H), 3.73 (s, 2H), 3.20–3.03 (m, 4H); ^{13}C NMR (62.9 MHz, DMSO-d_6) δ 129.33, 128.13, 119.28, 28.88, 26.95; DIP/MS (70 eV) m/z 286 (M^+, 76.7), 259 (57.6), 208 (100), 130 (36.0), 98 (66.4); exact mass calcd for $C_{18}H_{14}N_4$ 286.1218, found 286.1218.

Isolation of 20CN, the 1:1 Adduct between 5a and Fumaronitrile. Ketone **5a** (19.1 mg, 0.121 mmol) and fumaronitrile (99.7 mg, 1.27 mmol) were stirred at 20 °C in acetone (2 mL). After 3 days, TLC (1:1 Et_2O/hexane) showed some **5a** (R_f = 0.50) and a new spot at R_f = 0.05. Some insoluble bis-adduct **19CN** had also precipitated out of solution. The solvent was stripped off, and the residue was chromatographed on silica gel. The lower R_f material (10 mg, 35%) was isolated, and the ^{1}H NMR spectrum was consistent with the monoadduct: ^{1}H NMR (250 MHz, $CDCl_3$) δ 5.41 (m, 2H), 5.10 (m, 2H), 3.45 (s, 2H), 3.20 (m, 2H), 2.95–2.60 (m, 4H).

Spectrocopic Studies. UV–Vis Absorption Spectroscopy. General. Freshly prepared samples of ketone **5a** in 2-MTHF, methylcyclohexane, diethyl ether, toluene, or ethanol/methanol (4/1) were placed in Pyrex tubes which were attached *via* graded seals to rectangular (5 × 10 × 30 mm) quartz UV cells. Samples were deaerated either by bubbling with N_2 or by three freeze–pump–thaw cycles followed by sealing on the high-vacuum line. The samples were frozen by immersion in liquid nitrogen in either a square-sided Pyrex dewar, a cylindrical quartz dewar, or a round Pyrex dewar equipped with Suprasil flat quartz windows. Typically, the samples were irradiated using the 313-nm line of a 1000-W high-pressure Hg(Xe) lamp, using either a Pyrex filter or the monochromator. Quantitative UV–vis spectroscopic measurements were corrected by background subtraction of the appropriate solvent blank.

Short-Wavelength UV–Vis Measurement. Ketone **5a** (3.1 mg, 0.02 mmol) was dissolved in 10 mL of freshly distilled ether. A 1-mL aliquot of this solution was diluted to 5 mL, giving a final concentration of 0.4 mM. A portion of this sample was placed in a low-temperature UV cell and sealed under nitrogen. The sample was frozen in liquid nitrogen using the quartz dewar and examined by UV–vis prior to irradiation. The sample was then irradiated for short intervals (2–15 s) using the 200-W Hg lamp and a Pyrex filter. To maintain sample positioning during the photolysis, a mirror (Oriel Model 44170) was used to direct the light onto the sample. The spectrometer beam ports were covered during the photolysis in order to protect the instrument's photomultiplier.

Molar Absorptivity Measurements. All measurements were made on the Lambda 6 and were background corrected. Degassed samples of ketone **5a** in 2-MTHF or diethyl ether (1.5 mM, measured in a 0.10-cm solution cell on the basis of ϵ_{260} = 13 000[19] were placed in a low-temperature UV cell (0.3-cm path length) and frozen in liquid nitrogen in the square-sided Pyrex dewar. The samples were photolyzed (1000-W lamp, 313 nm) until there was no further increase in the 490-nm absorption band (~1 h). To ensure that the sample cells were perpendicular to the spectrometer beam, several absorbance measurements were made by rotating the samples slightly between scans. Absorbance measurements were also made in several different regions of the glass. The various readings differed by no more than 5%, and the lowest values for the optical densities at 490 nm were used to calculate the molar absorptivities. After thawing, the samples were assayed by capillary GC for residual **5a**.

Cryogenic UV–Vis Spectroscopy.[25] The Displex shroud was outfitted with four Suprasil quartz windows. A low-temperature UV cell[86] was mounted on the Displex, and a sample of ketone **5a** (6 mM in 2-MTHF) was introduced *via* syringe. The following operations were performed quickly in order to prevent thawing of the matrix and to minimize condensation. The sample and cryotip assembly were immersed in a dewar of liquid nitrogen. When the thermocouple had stabilized at 77 K, the dewar was removed and the Displex shroud was fitted over the sample. The shroud was opened to the vacuum line, and the Displex was turned on. When the temperature reached 14 K, an absorption spectrum was collected. The sample was then irradiated at 5-min intervals using the 200-W lamp, an Oriel 5145 filter, and a fiber-optic light pipe. A spectrum was collected after each photolysis interval.

Annealing UV–Vis Experiments. The Displex sample described above was annealed by setting the variable temperature controller to 100 K. After the purple color had faded, the sample was recooled to 77 K. UV–vis examination of the sample revealed a strong absorption at 380 nm with additional bands at 350 and 410 nm. In a separate experiment, a solution of **5a** in 2-MTHF (2 mM) was irradiated (313 nm) at 77 K for 2 h in a low-temperature UV cell. After UV–vis measurement of the 490-nm transient, the sample was annealed by withdrawing it briefly from the liquid nitrogen dewar. Dry helium was blown over the sample to prevent moisture condensation on the cell windows. When the purple color had faded (~30 s), the sample was reimmersed in the dewar and a spectrum was taken to monitor the 380-nm absorption. This process was repeated twice, allowing the sample to thaw for progressively longer times. Finally, the sample was thawed at room temperature, resulting in complete polymerization of the sample. Subsequent UV–vis examination at 77 K showed no absorption peaks above 300 nm. When a glass containing the 380-nm absorption (prepared as above) was photolyzed at 254 nm for 10 h, no visible change was observed in the matrix. Subsequent thawing of the sample led to polymer formation, and DIP/MS revealed no ions corresponding to m/z = 260.

Photobleaching of 1,2,4,5-Tetramethylenebenzene. A solution of **5a** in 2-MTHF (~2 mM) was placed in a low-temperature UV cell. The sample was degassed, sealed, and frozen in liquid nitrogen in a quartz dewar. The matrix was photolyzed for 1 h at 313 nm to generate the characteristic purple color of **4a**. After UV–vis inspection, the sample was then irradiated at 254 nm. The progress of the bleaching was monitored periodically by UV. After 2 h, the 490-nm transient in the section of glass under scrutiny was completely gone. Some purple color remained around the edges of the matrix. When the glass was thawed, a small amount of polymer formed. Capillary GC/MS analysis of the photolysate revealed only two peaks corresponding to unphotolyzed **5a** and to benzo[1,2:4,5]dicyclobutene (**17**). GC/MS retention times (T_i = 100 °C, t_1 = 5 min, rate = 10 °C/min, T_{max} = 240 °C, inj = 200 °C, det = 250 °C): **5a**, 7.21 min; **17**, 6.75 min. **17**: DIP/MS m/z 130 (M^+, 100), 129 (80.3), 128 (59.8), 127 (25.5), 115 (74.2), 102 (7.5), 89 (6.8), 77 (9.3), 63 (12.1).

Photolysis of Benzo[1,2:4,5]dicyclobutene (17). A 2-MTHF solution of benzo[1,2:4,5]dicyclobutene[87] (~1 mM) was sealed under N_2 in a low-temperature UV cell and irradiated at 77 K (1000-W lamp, 254 nm). After 2 h, UV inspection showed new absorptions extending out to 450 nm. The intensity of the new absorptions did not increase after an additional 2 h, and no absorption peaks attributable to **4a** were observed.

Excitation–Emission Spectroscopy. A solution of **5a** (~6 mM) in freshly distilled 2-MTHF was placed in a low-temperature quartz UV cell, and the sample was degassed and sealed in the usual manner. The sample was cooled to 77 K in the square-sided Pyrex dewar and irradiated for 1 h using the 313-nm line of the 1000-W lamp. The sample cell was rotated once during the course of the photolysis. The fluorescence spectrometer was designed such that the dewar could be lowered into the sample compartment through a hole in the cover. The sample cell was oriented at 45° with respect to the spectrometer excitation beam, and a nitrogen purge line was placed in the compartment to reduce moisture condensation. Emission spectra were collected by excitation of the 490-nm absorption, and excitation spectra were generated by monitoring the main emission at 670 nm. The sample was then thawed in the same manner as described for the annealing experiments, producing the 380-nm absorption (verified by UV–vis inspection). Emission (λ_{ex} = 380 nm) and excitation (λ_{em} = 470 nm) spectra were then collected for the 380-nm species. The excitation spectrum exhibited a broad shoulder from 350 to 400 nm and a maximum at 410 nm.

High Temperature Matrix Isolation of 1,2,4,5-Tetramethylenebenzene. Impregnation in Adamantane. Ketone **5a** (~15 mg) and adamantane (0.5 g) were intimately mixed and placed in a sublimator and then cooled in a dry ice/acetone bath while being evacuated on the high-vacuum line. When the pressure was $<10^{-4}$ Torr, the condenser was cooled to −78 °C and the solids were warmed to 40 °C with a water bath. After 1 h, the apparatus was flushed with N_2 and the sublimed material (~200 mg) was removed under nitrogen. A portion (10 mg) was dissolved in $CDCl_3$, and NMR analysis showed that the sublimate contained ~3.5% **5a** in adamantane. Approximately 100 mg of the sublimate was placed in an ESR tube, which was then degassed and sealed. The ESR sample was photolyzed at 77 K (1000-W lamp, 313 nm). After 10 min, the surface of the adamantane was noticeably pink; the part of the sample directly in front of the lamp was light brown. ESR examination of the sample at 77 K revealed a narrow (~100 G wide) signal at 3300 G. No half-field signal was observed. Rotating the sample in the ESR cavity did not affect the ESR signal. An estimate based on 1% conversion to **4a** gave a total number of spins >3.2 × 10.[17] The pink color was stable for 3 h at −150 °C but faded rapidly (<30 s) at −78 °C.

In Poly(methyl methacrylate). Nitrogen was bubbled through a 10-mL CH_2Cl_2 solution containing **5a** (5.7 mg, 0.036 mmol) and 255 mg

(86) For a description of this cell, see: Lahti, P. M. Ph.D. Thesis, Yale University, 1985, p 382.

(87) Prepared by Steven P. Schmidt according to the literature route. See: Gray, R.; Harruff, L. G.; Krymowski, J. P.; Boekelheide, V. *J. Am. Chem. Soc.* **1978**, *100*, 2892.

of poly(methyl methacrylate). After 20 min, the solution was injected by 250-μL aliquots into the polymer film deposition apparatus. Dry nitrogen was rapidly blown over the deposited solution. After the entire solution had been added (~2 h), the nitrogen flow was continued for an additional 2 h. The apparatus[23b] was then attached to the high-vacuum line, and the film was pumped on at 2×10^{-4} Torr for 45 min. Dry nitrogen was rapidly blown over the deposited solution. After the entire solution had been added (~2 h), the nitrogen flow was continued for an additional 2 h. The apparatus was then attached to the high-vacuum line, and the film was pumped on at 2×10^{-4} Torr for 45 min. The apparatus was vented under nitrogen in a glovebag, and the polymer film was broken up into small pieces. Photolysis (313 nm) of film pieces at 77 K produced a purple/brown color which persisted at −78 °C for several hours. The color was stable at −61 °C ($CHCl_3/CO_2$) but faded at −50 °C (CH_3CN/CO_2). The film samples turned yellow briefly during the thawing. A film sample (~0.5 × 2 × 5 mm) was placed in a flat-sided ESR cell, which was then sealed under N_2 and photolyzed at 77 K, generating the purple color and a weak absorption at 490 nm (O.D. ~ 0.05–0.08). The absorption bands at 575 nm and 620 nm were not detected. The color persisted in the film at 195 K, and no change in the absorption spectrum was observed at the higher temperature. ESR examination of the film sample at 195 K revealed only a weak, narrow signal, which did not change when the sample was reoriented in the sample cavity. An estimate gave 6.02×10^{17} biradical molecules for this sample, on the basis of a film area of 0.1 cm^2 and $\epsilon_{490} = 5000$ M^{-1} cm^{-1}.

Electron Spin Resonance Spectroscopy.[88] **General.** ESR experiments were performed on freshly prepared samples of labeled ketone **5a** (0.001–0.059 M) in 2-MTHF, diethyl ether, methylcyclohexane, adamantane, or poly(methyl methacrylate). The samples were placed in Wilmad SQ-707 or SQ-727 Suprasil quartz tubes. Quantitative ESR/UV–vis experiments were conducted with a Wilmad WG-808-Q ESR cell with a Suprasil flat section. This cell had a path length of 0.5 mm. Photolyses were carried out at 77 K with the 1000-W high-pressure Hg(Xe) lamp at either 313 nm or with Pyrex filtering. Typically, the samples were irradiated outside the ESR probe in order to maximize conversion. They were then quickly transferred to the precooled (10 K or 77 K) cavity for ESR examination. In one experiment, a sample tube was irradiated inside the ESR cavity using the full output of the 200-W Hg lamp and spectra were collected during photolysis. Typical instrument parameters were as follows: receiver gain $1.25 \times 10^2 - 2.5 \times 10^4$, modulation amplification $2.0 \times 10^{-1} - 2.0 \times 10^1$, time constant 0.1 – 0.3 s, scan rate 2 – 16 min, microwave power 0.1 – 5.0 mW. In only one case was an ESR signal wider than the 100-G signal observed, and a control experiment established that it originated from an impurity in the 2-MTHF.

Thawing and Rephotolyzing Experiments. In the repetitive photolysis experiments, purple samples were removed from the ESR cavity and allowed to thaw at room temperature. The samples were then refrozen and rephotolyzed at 77 K. If any biradical was formed (as indicated by the reappearance of the purple color), the process was repeated. The ESR spectra of samples not containing the purple color consisted of a strong, featureless transition at 3280 G. No half-field signal was observed when a sample was examined at 10 K.

Photobleaching ESR Experiment. A solution of ketone **5a** (~10 mM) in 2-MTHF was degassed by bubbling with N_2 at 0 °C for 30 min. A 0.5-mL aliquot was placed in an SQ-727 ESR tube, and the sample was degassed and sealed in the usual manner. The tube was frozen at 77 K in the square Pyrex dewar and irradiated at 313 nm. After 2 h, the intensely colored purple sample was transferred to the precooled (10.6 K) ESR cavity and spectra were collected for both the $\Delta m_s = 1$ and $\Delta m_s = 2$ regions. The sample was then transferred to a quartz dewar and irradiated with the full output of the 1000-W Hg(Xe) lamp. The tube was rotated and repositioned during the course of the photolysis in order to bleach all of the purple color. After 5 h, the sample was examined by UV–vis to confirm the complete absence of the 490-nm absorption. The tube was then reexamined by ESR at 10.6 K. The same instrument settings were used to examine the sample both before and after the photobleaching. No change in the signal intensity of the half-field transition was observed, and the intensity of the $\Delta m_s = 1$ transition at 3280 G was considerably larger.

A sample which had been photobleached as described above was stored at 77 K for 2 weeks. No change in the ESR signal was apparent after this time, and the purple color did not return to the sample even after 2 months at 77 K.

The possibility that the ESR signal(s) arose from TMB photoproducts was investigated by photolyzing (254 nm) a 2-MTHF glass of benzo[1,2:4,5]dicyclobutene (**17**). However, ESR examination of this sample at 10 K revealed only weak, solvent-derived signals in the $\Delta m_s = 1$ region, and no half-field transitions were observed.

Tandem ESR/UV–Vis Experiment. Ketone **5a** (5 mg, 0.032 mmol) was dissolved in methylcyclohexane (5 mL, freshly distilled from CaH_2), and 100 μL of this solution was placed in the SQ-808-Q flat-sided ESR cell. The sample was covered with nitrogen and sealed. The sample was then photolyzed (313 nm) at 77 K in the square Pyrex dewar. After 30 min, the optical density of the 490-nm absorption (~0.37) was used to estimate a biradical concentration of 1.5 mM (on the basis of $\epsilon_{490} = 5000$). ESR measurement at 77 K showed only a narrow impurity signal. Reexamination of the sample by UV–vis showed that no diminution in biradical concentration had occurred during transport between the spectrometers.

Photosensitized Photolyses. ESR samples of **5a** (~10 mM) and either benzophenone or acetophenone (0.3 M) in 2-MTHF were sealed and irradiated at 77 K for 30 min using the 365-nm line of the 1000-W lamp. When examined by ESR at 10 K, only weak solvent signals were observed for both samples. When the acetophenone sample was photolyzed at 313 nm for 30 min, a light purple color was generated. Subsequent ESR examination at 10 K revealed a narrow signal at 3280 G and a weak half-field transition at 1650 G.

Low-Temperature Solid-State CP MAS ^{13}C NMR Spectroscopy. General Procedure. Freshly prepared solutions of *di-^{13}C*-labeled ketone **5b** (0.09–0.10 M) in 2-MTHF or toluene were placed in standard 5-mm Pyrex NMR tubes which had been "precrimped" for ease in sealing on the high-vacuum line. The samples were degassed (three freeze–pump–thaw cycles) and sealed. Great care was taken to center the seal with respect to the tube, since an unbalanced tube would not spin well. The total sample volume was kept between 100 and 125 μL to ensure that the entire sample would be immersed in liquid nitrogen when the tube was sealed and placed in the NMR turbine. Once loaded into the spinner turbine, the samples were frozen in liquid nitrogen. The samples were then quickly transferred to the precooled (77 K) probe and "spun up". Solid-state ^{13}C CP MAS NMR spectra (25.15 MHz) were collected at 77 K at spinning rates from 1.9 to 2.4 kHz. Spectra were recorded at multiple spin rates to assign spinning sidebands.

After a spectrum of the precursor (**5b**, observed at 105 ppm in both 2-MTHF and toluene) had been collected, the NMR samples were photolyzed at 77 K using the 1000-W Hg(Xe) lamp at 313 nm, or they were Pyrex-filtered. In practice, the NMR tubes were attached to a copper wire with Teflon tape so that they could then be lowered into the liquid nitrogen dewar. The samples were rotated periodically during the course of the photolysis to maximize the biradical concentration. Irradiating the samples for more than 1 h did not lead to higher conversions, which ranged from 30 to 45% in 2-MTHF and 10 to 20% in toluene (as measured by NMR). One experiment using the Rayonet photoreactor (300 nm) resulted in substantially lower conversion. Following photolysis, the purple samples were transferred back into the NMR rotor. Great care was taken to remove all frost from the surfaces of the sample assembly, since ice could cause the rotor to bind up in the probe, resulting in premature thawing of the sample. The samples were then returned to the NMR probe, and spinning was started.

After NMR observation of the 113 ppm intermediate, the samples were removed from the probe to visually confirm the presence of the purple color. The samples were then annealed in an isopentane/N_2 slush bath at a temperature of 120 K to quench the biradical. Reexamination by NMR showed that the 113 ppm peak was absent. No other new NMR absorptions which could be attributed to TMB products were observed, even when the matrices clearly contained the 380-nm chromophore. The samples were then thawed at room temperature and refrozen, and NMR spectra were collected. The thawed toluene samples exhibited broad peaks at 30 ppm.

Estimation of Percent Conversion by UV–Vis Absorption Spectroscopy. A 0.1 M solution was prepared by dissolving **5a** (15.8 mg, 0.1 mmol) in 1 mL of freshly distilled 2-MTHF. A small amount of polymeric material was removed by filtering the solution through a plug of glass wool. The solution was placed in a low-temperature cell (2-mm path length) and sealed. The sample was then photolyzed for 1 h at 77 K under conditions identical to those used in the CP MAS experiments (1000-W lamp, Pyrex filter, frequent sample rotation). When the sample was examined by UV–vis, the 490-nm peak was off-scale. The optical density of the 620-nm absorption (3.36) was used to estimate a biradical concentration of ~34 mM (34% conversion on the basis of $\epsilon_{620} = 500$ M^{-1} cm^{-1}). The actual percent conversion may have been slightly higher due to the polymer contribution to the original sample weight.

(88) We thank L. C. Bush for participation in early ESR experiments.

Long-Term Storage Experiment. A purple sample of biradical **4b** in 2-MTHF which had been previously examined by CP MAS NMR was stored in a 10-L liquid nitrogen dewar. To facilitate handling, the sample tube was not removed from the rotor during storage. After 1 week, the sample was reexamined by NMR. Some thawing had occurred, possibly during transfer, which resulted in a decrease (~20%) in the intensity of the 113 ppm absorption. However, after an additional 10 days at 77 K, no further change in the NMR signal intensity was observed.

Preparation of Labeled Polymer. A solution of ketone **5b** (0.1 M) in 350 μL of 2-MTHF was placed in an NMR tube, which was then sealed on the high-vacuum line. The sample was irradiated in the Rayonet photoreactor at ambient temperature using the 300-nm lamps. After 90 min, the tube was opened and the 2-MTHF was syringed away from the polymer. The polymer was washed with diethyl ether (3 × 200 μL), dried under vacuum, and placed in a 1-in. NMR tube. A glass wool plug was used to keep the polymer in place while spinning in the CP MAS NMR probe. The solid-state NMR (298 K) of this material exhibited a broad absorption at 30 ppm and a weaker absorption at 70 ppm.

Concentration Dependence of the Thermal Reaction between 5a and Diethyl Fumarate. Three NMR samples were prepared by adding 200 μL of a 0.07 M CD_3CN solution of **5a** to 200 μL each of 1.0 M diethyl fumarate, 2.0 M diethyl fumarate, and CD_3CN. *p*-Dichlorobenzene (~5 mg) was added to each tube as an internal standard. The three tubes and a fourth tube containing only CD_3CN were degassed (three freeze–pump–thaw cycles) and sealed on the high-vacuum line. The tubes containing **2** were stored at 0 °C while awaiting their turn for examination by NMR. The CD_3CN blank was used to equilibrate the NMR probe to 333 K, and a microprogram was written to automate the NMR acquisitions.

The tubes containing **5a** and diethyl fumarate were each examined in turn, and the reaction was monitored for at least 3 half-lives. During the reaction, new methylene signals attributed to the monoadduct **20E** appeared at 5.39 and 5.07 ppm. The disappearance of **5a** was measured by comparing the integrated area of its methine peak at 5.46 ppm against the area of the *p*-dichlorobenzene standard at 7.35 ppm. The peaks being monitored were singlets, and the peak printout program of the NMR spectrometer was used to provide accurate integrations. The tube containing only **5a** was measured for as long as the other tubes, although it showed little change during the course of the experiment. In the tube containing 0.5 M fumarate, the growth of the monoadduct peak at 5.07 ppm was also monitored.

Thermolysis of 5a in DMSO-d_6. NMR samples of ketone **5a** (0.038 and 0.10 M) in DMSO-d_6 were degassed and sealed and then thermolyzed in the 250-MHz NMR probe (preheated to 373 or 383 K). The NMR acquisitions were automated as described above, with spectra collected either every 20 min (373 K) or every 10 min (383 K). The ketone concentration was monitored by comparing the area of its methine peak at 3.57 ppm with the small water peak at 2.93 ppm. The disappearance of **5a** was followed for at least 3 half lives.

Reactions of Photochemically Generated TMB in the Presence of Olefins. Diethyl Fumarate. Ketone **5a** (20 mg, 0.126 mmol) was dissolved in 10 mL of a 0.5 M $CDCl_3$ solution of diethyl fumarate (40 equiv). The solution was placed in a 15-mL centrifuge tube and purged with N_2 at 0 °C (30 min). The tube was then photolyzed for 2 h in the Rayonet (300 nm, 0 °C). The solution remained homogeneous during the reaction. The solvent was removed *in vacuo*, and the residue was washed with 1:1 pentane/ether (4 × 5 mL) to remove the excess diethyl fumarate. The product (22 mg, beige solid) was soluble in $CDCl_3$. No 2:1 adduct **19E** was detected when the sample was analyzed by capillary GC or DIP/MS: ^1H NMR (250 MHz, $CDCl_3$) δ 6.8 (br, ~1H), 4.15 (br, ~2H), 3.3 2.0 (br, ~5H), 1.3 (br, ~3H); FTIR ($CDCl_3$) (cm^{-1}) 1750, 1436, 1399, 1337, 1299, 1260, 1161, 1030.

Fumaronitrile. 2,3,10,11-Tetracyano-1,2,3,4,6,7,9,10,11,12,14,15-dodecahydrodinaphtho[a,e]cyclooctene (23CN). Ketone 5a (20 mg, 0.127 mmol) and fumaronitrile (97 mg, 1.25 mmol) were dissolved in $CHCl_3$ (5 mL) in a 15-mL centrifuge tube. The tube was fitted with a serum cap, and the solution was degassed by bubbling with N_2 at 0 °C for 30 min. The solution was then photolyzed at 0 °C (Rayonet, 300 nm) for 2 h, leading to the formation of a precipitate. Diethyl ether (5 mL) was added, and the solution was centrifuged. The solvent was decanted, and the solid was washed with two more aliquots of ether (5 mL, spinning down after each washing), giving 18.0 mg (68%) of beige powder: mp >200 °C; ^1H NMR (250 MHz, DMSO-d_6) δ 6.78 (s, 1H), 3.64 (m, 1H), 3.15–2.90 (m, 2H), 2.97 (s, 2H); ^{13}C NMR (62.9 MHz, DMSO-d_6) δ 138.10, 129.25, 128.15, 119.45, 33.48, 28.91, 26.95; DIP/MS (70 eV) *m/z* 416 (M^+, 28.0), 389 (57.7), 362 (100), 236 (63.6), 208 (70.5); exact mass calcd for $C_{28}H_{24}N_4$ 416.2001, found 416.1986.

Effect of Fumaronitrile Concentration on Product Composition in the Photolysis of 5a. A 0.1 M $CDCl_3$ stock solution of **5a** and a 1.25 M solution of fumaronitrile in $CHCl_3$ were used to prepare two 5-ml samples as follows:

sample no.	ketone **5a** vol (mL)	[**5a**] (mM)	fumaronitrile vol (mL)	[trap]	$CHCl_3$ vol (mL)
1	1.0	20	0.4	0.1	3.6
2	1.0	20	4.0	1.0	0

All subsequent handling of the solutions was done at 0°°C. The two samples were placed in 15-mL centrifuge tubes and deaerated by purging with nitrogen for 30 min. The two tubes were placed in an ice bath and irradiated for 2.5 h (Rayonet, 300 nm). The cooling bath was replenished every 30 min. During the photolysis, the products precipitated out of solution. The two samples were then subjected to identical workups. The solvent was evaporated, and the residue was taken up in diethyl ether (5 mL). This solution was centrifuged, and the ether was decanted away from the precipitate. The solids were washed twice more with ether (5 mL) and then dried under vacuum.

Sample 1: 14.5 mg; NMR analysis (DMSO-d_6) showed only the 2:2 adduct **23CN**; yield 70%.

Sample 2: 19.5 mg; NMR analysis showed this to be a 5.3/1 mixture of 2:1 and 2:2 adducts **19CN** and **23CN**, on the basis of the integration of their phenyl protons at 6.95 and 6.78 ppm, respectively; mass balance 75%. A small peak at 7.02 ppm in this spectrum remains unassigned.

A separate control experiment showed no thermal reaction between 0.05 M **5a** and 1.0 M fumaronitrile after 4.5 h at 0 °C and <10% reaction after an additional 20 hours at 25 °C.

Maleic Anhydride. A 0.5 M solution of maleic anhydride in $CDCl_3$ (5 mL) was placed in a 7 × 100-mm NMR tube, and the solution was bubbled with N_2 at 0 °C for 1 h. Ketone **5a** (26.5 mg, 0.17 mmol) was then added, and nitrogen bubbling was continued for an additional 30 min. A 0.5-mL aliquot was taken and examined by NMR, which showed a trap/ketone ratio of ~16:1. This NMR sample was kept at 0 °C while the large tube was photolyzed in the Rayonet (300 nm, 0 °C). After 90 min, large amounts of precipitate had formed in the tube. NMR analysis of a 0.5-mL portion of the solution showed >98% conversion of **5a** while the unphotolyzed tube showed no reaction between **5a** and the maleic anhydride. The photolyzed solution was centrifuged, and the supernatant was removed by pipet. The precipitate was washed with $CHCl_3$ (3 × 2 mL), centrifuging after each washing. The product (43 mg, 78%) was dried under vacuum. NMR analysis (DMSO-d_6) showed only 2:1 adduct.

Using 2 equiv of trap, maleic anhydride (31 mg, 0.32 mmol) was added to 2 mL of a 0.08 M $CDCl_3$ solution of **5a** in an NMR tube. NMR analysis indicated a 2:1 trap/ketone ratio. After degassing, the sample was photolyzed (300 nm, 0 °C) for 1 h. NMR examination of the photolysate showed no **5a** and some maleic anhydride. Diethyl ether (2 mL) was added and the solution was centrifuged. The precipitate was washed with ether (3 × 2 mL). The product (26 mg, beige powder) was slightly soluble in DMSO-d_6. ^1H NMR showed only the 2:1 adduct. Mass spectroscopic analysis also showed a peak at $m/z = 456$. The exact mass of this ion was 456.1592, consistent with a 2:2 adduct between **4a** and maleic anhydride (calculated for $C_{18}H_{14}O_6$: 456.1573).

Photolyses of **5a** were also conducted in the presence of acrylonitrile (up to 20 equiv), styrene (17 equiv), and dimethyl maleate (20 equiv). The products of these photolyses remain uncharacterized.

Reaction of Oxygen with Photochemically Generated TMB. Ketone **5a** (23 mg, 0.145 mmol) was dissolved in oxygen-saturated $CHCl_3$ (10 mL) in a 25-mL Pyrex test tube. The tube was fitted with a serum cap, and oxygen was bubbled through the solution *via* an 18-gauge needle. The tube was placed in an ice/water bath, and oxygen bubbling was continued while the solution was photolyzed (1000-W lamp, monochromator at 313 nm). The solution remained homogeneous throughout most of the photolysis. Toward the end of the photolysis (3 h), the solution became slightly turbid. Thin-layer chromatography (1:1 ether/hexane) showed no **5a** and a new spot at $R_f = 0.85$. This spot was isolated by column chromatography (1:1 ether/pentane), giving 22.6 mg of material. NMR analysis showed this to be a 1.8:1 mixture of the fused di- (55% yield) and bridged monoperoxides (30%). This mixture was combined with the material from a second run, and the components were separated by column chromatography (1:4 ether/pentane).

2,3-Dioxa-5,6,7,8-tetramethylidenebicyclo[2.2.2]hexane (28): $R_f = 0.5$; ^1H NMR (250 MHz, $CDCl_3$) δ 5.57 (s, 2H), 5.16 (s, 2H), 4.83 (s, 1H); ^{13}C NMR (62.5 MHz, $CDCl_3$) δ 140.39, 109.73, 84.14; GC/MS (70 eV) *m/z* 162 (M^+, 19.5), 133 (22.6), 105 (28.3), 91 (100), 65 (21.2), 51 (12.7); exact mass calcd for $C_{10}H_{10}O_2$ 162.0681, found 162.0658.

5,6,12,13-Tetroxatricyclo[8.2.0.0^{3,8}]tetradeca-1,3(8),9-triene (29) (R_f = 0.25). The spectroscopic properties of the diperoxide were identical to those previously reported:[42] ^{1}H NMR (250 MHz, $CDCl_3$) δ 6.89 (s, 1H), 5.21 (s, 4H); ^{13}C NMR (62.5 MHz, $CDCl_3$) δ 130.7, 120.2, 71.0; GC/MS (70 eV) *m/z* 194 (M^+, 10.8), 176 (22.2), 167 (35), 162 (15), 149 (100), 105 (12), 91 (25), 57 (28).

Flash Vacuum Pyrolysis of 5a. Formation of 17. A quartz pyrolysis tube was packed with quartz helices, and ketone **5a** (50 mg, 0.19 mmol) was placed in the inlet flask. The sample was cooled to 77 K while the pyrolysis apparatus was evacuated to $<1 \times 10^{-6}$ Torr. The furnace was heated to 410 °C, and the collection finger was filled with liquid nitrogen. A warm water bath (40 °C) was used to sublime the sample. After 1 h, a heat gun was used to sublime the remaining material. Some polymeric material remained behind in the inlet flask. The collection finger was then allowed to warm to room temperature. After disassambly of the apparatus, the surface of the cold finger was rinsed with diethyl ether and the collected rinsings were concentrated, giving 18 mg (44%) of a white solid. This was taken up in $CDCl_3$ and ^{1}H NMR analysis showed this to be a nearly pure sample of benzo[1,2:4,5]dicyclobutene (**17**). ^{1}H NMR (250 MHz, $CDCl_3$) δ 6.80 (s, 1H), 3.14 (s, 4H).

Laser Flash Photolysis Studies. Solutions of **5a** in HPLC-grade solvents (chloroform, toluene, or acetonitrile) were prepared and had optical densities of 0.3–0.6 at the 308-nm laser line. This required concentrations of 1–2 mM. Solutions were placed in 7- × 7-mm static cells and deaerated by purging with dry nitrogen for 20 min.

Dimerization Kinetics. All kinetic studies were run at 291 K. Typically, 8–10 laser shots were sufficient to generate decay plots for the 490-nm transient, producing optical densities of 0.03–0.06. This corresponded to initial transient concentrations of $\sim 1 \times 10^{-5}$ M. The decay traces (see Figure 13) fit a second-order rate law with correlation coefficients >0.99. The decay of the absorptions at 575 and 620 nm were also measured, although the low optical densities at these wavelengths made accurate fits difficult. Also, the dimer growth (absorption at 380 nm) was measured for each sample. Neutral density filters of varying transmittance (100, 70, 25, 15, and 5%) were interposed between the laser and sample and established that the kinetic order and the rate constant were not dependent on the initial transient concentration. The dimerization rate constants $2k_t$ were derived from the relationship $2k_t = k_{obs}\,\epsilon l$, on the basis of ϵ_{490} = 5000 M^{-1} cm^{-1} and l = 0.7 cm, where k_{obs} is the reciprocal of the lifetime at 1 M concentration of the transient.

Oxygen Quenching of Flash-Photolytically Generated 1,2,4,5-Tetramethylenebenzene. Solutions of **5a** in $CHCl_3$, toluene, and CH_3CN were prepared in 7- × 7-mm static cells as described above. The samples were bubbled with oxygen at room temperature for 20 min prior to the flash photolysis experiment. Samples containing varying amounts of oxygen were prepared by bubbling chloroform solutions of **5a** with 100% O_2, air (prepurified, 21% O_2), and 1% O_2/N_2. In each case, Henry's law was assumed when calculating the final oxygen concentration. The lifetime of the 490-nm transient in oxygenated solvents was considerably shorter ($\sim 1\,\mu s$) than in deaerated solutions ($\sim 20\,\mu s$). The decay of the absorption could be fitted to a first-order rate law with $R \geq 0.995$.

Transient Solution Spectra of 1,2,4,5-Tetramethylenebenzene. A 100-mL solution of ketone **5a** in $CHCl_3$ was prepared and had an optical density of 0.3 at 308 nm ($\sim$1.3 mM). To minimize light scattering by the polymeric products, this solution was used in a 7- × 7-mL flow cell with a flow rate of $\sim$2 mL/min. Nitrogen was bubbled into the reservoir containing the sample solution. A transient spectrum at 291 K was obtained by collecting delay traces at 4-nm increments from 675 to 320 nm (eight laser shots per wavelength). Windows on the transient decay were set at 0.3, 7.0, 16.6, and 33.2 μs.

A second solution of **5a** was used to generate a transient spectrum of **4a** in oxygen-saturated $CHCl_3$. The same conditions as those described above were used except oxygen was bubbled into the solution reservoir. The shorter lifetime of the 490-nm transient in O_2-saturated solution required that the decay windows be set at 0.25, 2.96, 7.92, and 17.4 μs.

Attempted Quenching of TMB with Trapping Agents. Quenching of the 490-nm transient was attempted by the addition of aliquots taken from 1.0 M stock solutions of diethyl fumarate, fumaronitrile, and maleic anhydride. In no case was any quenching of the 490-nm absorption observed. The maximum trap concentrations used were 0.4 M (diethyl fumarate), 0.2 M (fumaronitrile), and 0.1 M (maleic anhydride).

Acknowledgment. We thank the U.S. National Science Foundation (CHE-9119957 and 9018455) and the Swiss National Science Foundation for grants in support of this work. The participation of D. M. Birney and L. C. Bush in some of the spectroscopic experiments is gratefully acknowledged.

Supplementary Material Available: Description of low-temperature IR and UV–vis spectroscopic characteristics of **4a** and the effect of trapping agent concentration in photolysis of **5a** (9 pages). Ordering information is given on any current masthead page.